ИНСТИТУТ
ПО ОРГАНИЧНА ХИМИЯ
С ЦЕНТЪР ПО ФИТОХИМИЯ
Българска Академия на науките

ОТЧЕТ ПО ПРОЕКТ ЗА НАУЧНО И КАРИЕРНО РАЗВИТИЕ

НАЦИОНАЛНА ПРОГРАМА „МЛАДИ УЧЕНИ И ПОСТДОКТОРАНТИ“ II ЕТАП

Тема: “Взаимодействия на йонни течности на основата на фармацевтично-активни съединения и албумин“

Участник: 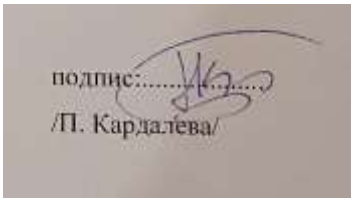

/маг. биолог Пролетина Кардалева/

Научен ръководител: 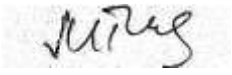

/доц. д-р Мая Гунчева/

София, февруари, 2021 г.

Въведение (включва анотация на представения проект, цели, работна програма, предвидени дейности - до 2 стр.)

Създаването на нови лекарствени формулировки е обект на засилен интерес от страна на фармацевтичната индустрия. Чрез тях се цели повишаване на стабилността, водоразтворимостта и съответно бионаличността на фармацевтично-активната съставка и/или да се повлияе на продължителността на действие и да се намали токсичността на лекарството. Значителна част от синтетичните и природни съединения, които показват много висока биологична активност в ин витро изследвания, не успяват да достигнат до клиничната практика заради ниска разтворимост при физиологични условия. Освен това фармацевтично-активни съединения имащи кристална структура могат да съществуват в няколко полиморфни форми, които притежават различни физикохимични характеристики и различна терапевтична активност. Това също е предизвикателство пред фармацевтичната индустрия. Превръщането на фармацевтично-активни съединения в йонни течности (ЙТ) е обект на засилен интерес от страна на научната общност и показва значителен потенциал за създаване на нови лекарствени форми.

Обект на изследване на настоящия проект са серии ЙТ, съдържащи катиони алкилови естери на аминокиселини и аниони – нестероидни противовъзпалителни и/или болкоуспокояващи средства като кетопрофен (KETO), ибупрофен (IBU), напроксен(NAP) и салицилова киселина(SA). Цел на проекта е да се установи, как новите лекарствени форми под формата на ЙТ си взаимодействат и се свързват с албумин. Както и какъв е ефекта на тези съединения върху стабилността на албумина. Албуминът е основен транспортен протеин при човека и бозайниците. Изучаването на взаимодействията му с целевите ЙТ ще даде предварителна информация за усвояването, метаболизма и токсичността им, както и за потенциала им за бъдещо лекарствено приложение. В изследването е използван говеждият серумен албумин (BSA), който е високо хомоложен (до 76%) на човешкия серумен албумин и често се използва като модел в ин витро изследвания.

*e-mail: proletina.kardaleva@orgchm.bas.bg

През първия етап на настоящия проект бяха изследвани серии ЙТ, съдържащи анион кетопрофен.

Фокусът на изследванията на втория етап са серии ЙТ, съдържащи напроксен и ибупрофен.

За втория етап на проекта бяха поставени следните задачи:

а) Да се определят константите на свързване, броят на свързващите места и термодинамичните параметри на BSA и целевите ЙТ.

б) Да се проследи ефекта на целевите ЙТ върху вторичната и третичната структура на BSA.

в) Да се проследи ефекта на целевите ЙТ върху термостабилността на BSA.

г) Актуализиране на литературната справка за синтеза и ефективността на ЙТ на основата на нестероидни противовъзпалителни и болкоуспокояващи съединения.

д) Разпространение на резултатите. Оформяне на публикации. Участие в научни мероприятия.

е) Оформяне на междинния и на крайния отчет.

Използвани са следните подходи:

За определяне на параметрите на свързване и термодинамиката на взаимодействията на BSA с ЙТ е използвана изотермична титриметрична калориметрия.

За проследяване на ефекта на ЙТ върху вторичната и третичната структура на BSA са използвани инфрачервена спектроскопия и флуоресцентна спектроскопия.

За установяване на ефекта на ЙТ върху термодинамичната стабилност на BSA е използвана диференциална сканираща калориметрия.

*e-mail: proletina.kardaleva@orgchm.bas.bg

Резултати и обсъждане (до 10 стр.)

През настоящия етап на проекта бяха изследвани 6 ЙТ, съдържащи анион ибупрофен и 5 ЙТ, съдържащи анион напроксен. Структурите на изследваните съединения са показани на схема 1.

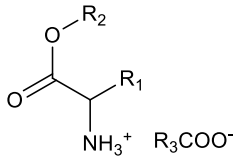

R_1	R_2	R_3	Означение
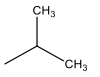	-CH_2CH_3	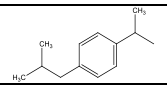	[L-ValOEt][IBU](1)
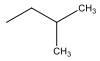	-CH_2CH_3	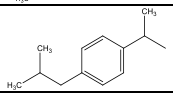	[L-LeuOEt][IBU](2)
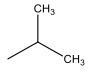	-$CH_2CH_2CH_3$	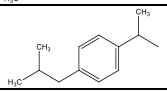	[L-ValOPr][IBU](3)
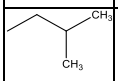	-$CH_2CH_2CH_3$	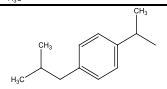	[L-LeuOPr][IBU](4)
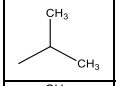	-$CH(CH_3)_2$	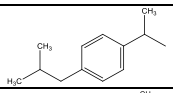	[L-ValOiPr][IBU](5)
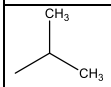	-$CH_2CH_2CH_2CH_3$	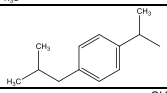	[L-ValOBu][IBU](6)
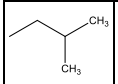	-CH_2CH_3	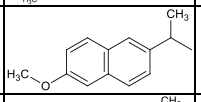	[L-LeuOEt][NAP](7)
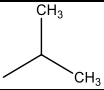	-CH_2CH_3	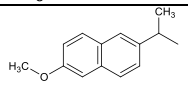	[L-ValOEt][NAP](8)
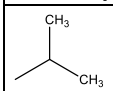	-CH $(CH_3)_2$	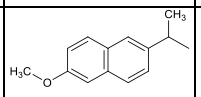	[L-ValOiPr][NAP](9)
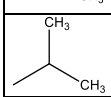	-$CH_2CH_2CH_3$	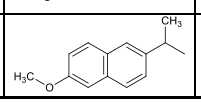	[L-ValOPr][NAP](10)

*e-mail: proletina.kardaleva@orgchm.bas.bg

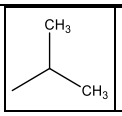	-$CH_2CH_2CH_2CH_3$	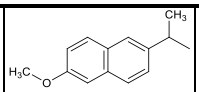	[L-ValOBu][NAP](11)

Схема 1Изследвани йонни течности

Изотермичната титриметрична калориметрия е надежден и информативен метод за изследване на взаимодействията между макромолекули и лиганди. Той позволява да се определи стехиометрията на свързване, константи на асоциация и дисоциация, и термодинамичните параметри. На фиг. 1 за илюстрация е показана калориметричната титрационна крива за сързване на L-ValOiPr][NAP] в молекулата на BSA.

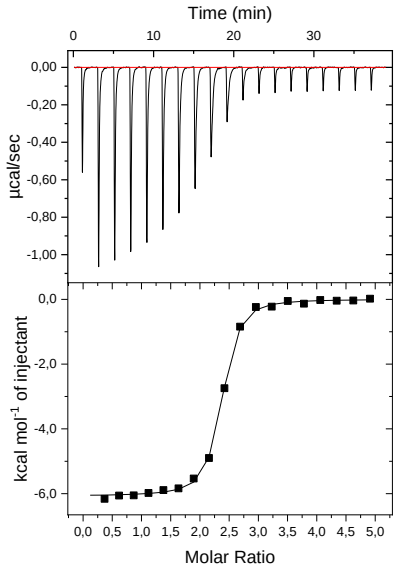

Фигура 1. Изотерма на свързване, получена при титруване на BSA (32,5 µM) и [L-ValOiPr][NAP] (0,45 mM) (горен панел) и обработването й по модел – един тип независими подцентрове (долен панел). T= 25ºC.

Подобни изотермални титриметрични криви са получени за всички комплекси на BSA с ЙТ и получените резултати са обобщени в таблица 1 за ЙТ с анион напроксен и в таблица 2 за ЙТ с анион ибупрофен.

Таблица 1. Брой свързващи места (n), константата на свързване (K_a) и термодинамичните параметри за взаимодействията на NAP/NAP-ЙТ с BSA, pH 7,4; 25ºC.

*e-mail: proletina.kardaleva@orgchm.bas.bg

Комплекс	n	K_a (μM^{-1})	ΔH (kcal/mol)	ΔS (kcal/mol)	ΔG (kcal/mol)
BSA-NAP	1	11,2	-13,16	-11,9	-9,61
BSA-[L-LeuOEt][NAP]	1,1	12,3	-12,54	-9,63	-9,68
BSA-[L-ValOEt][NAP]	1,1	15,6	-13,63	-13,2	-9,69
BSA-[L-ValOiPr][NAP]	2,2	3,5	-5,98	9,9	-8.83
BSA-[L-ValOPr][NAP]	0,8	12,3	-16,45	-22,2	-9,84
BSA-[L-ValOBu][NAP]	0,8	12,2	-16,6	-23,3	-9,38

Таблица 2. Брой свързващи места (n), константата на свързване (K_a) и термодинамичните параметри за взаимодействията на IBU/IBU-ЙТ с BSA

Комплекс	n	K_a (μM^{-1})	ΔH (kcal/mol)	ΔS (kcal/mol)	ΔG (kcal/mol)
BSA-IBU	1,0	0,36	-9,32	-1,65	-7,65
BSA-[L-ValOEt][IBU]	0,9	0,2	-9,23	-1,99	-7,24
BSA-[L-LeuOEt][IBU]	0,9	0,2	-9.,8	-2,56	-7,22
BSA-[L-ValOPr][IBU]	1,3	0,2	-11,95	-4,71	-7,24
BSA-[L-LeuOPr][IBU]	0,9	0,17	-17,04	-9,89	-7,15
BSA-[L-ValOiPr][IBU]	1,0	0,34	-9,26	-1,71	-7,55
BSA-[L-ValOBut][IBU]	0,9	0,12	-11,5	-4,38	-7,61

Както се вижда от резултатите, напроксенът и неговите ЙТ се свързват с BSA с до два порядъка по-силен афинитет спрямо ибупрофена и неговите ЙТ. Формирането на всички комплекси на BSA с ЙТ е спонтанен процес (ΔG<0) и вероятно е съпроводено с конформационни промени в албумина при свързване на лигандите. С изключение на [L-ValOiPr][NAP], при всички останали ЙТ и изходните съединения, напроксен и ибупрофен свързването се благоприятства от енталпията. Тези комплекси са стабилизирани чрез Ван дер Ваалсови взаимодействия и водородни връзки между лиганда и макромолекулата. За образуването на комплекса BSA-[L-ValOiPr][NAP] съществен принос имат и ентропията, и енталпията. В този случай всяка молекула албумин пренася две молекули лиганд. При ЙТ на напроксена и ибупрофена с [L-ValOBu] и [L-ValOPr] производните се свързват със стехиометрия по-малка от 1:1, което според нас се дължи на свързване на съединенията в свързващ подцентър („джоб“) близо до повърхността на протеина, което позволява молекулата на напроксена/ибупрофена да се свързват чрез естерната си група с една молекула албумин, а с ароматния фрагмент да участват в хидрофобни взаимодействия с друга молекула албумин. Тези хипотези са доказани чрез молекулна динамика, резултати коментирани по-подробно в излязлата от

*e-mail: proletina.kardaleva@orgchm.bas.bg

печат публикация през настоящия етап на проекта.

Образуването на комплекси на албумин с ЙТ с анион ибупрофен беше проследено и спектрофлуориметрично. С повишаване на концентрацията на лигандите флуоресценцията, дължаща се главно на триптофиловите и тирозиновите остатъци се погасява (Фиг. 2)

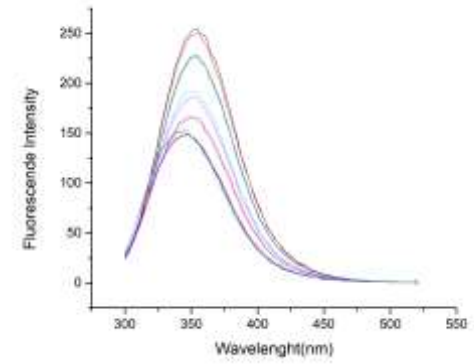

(а)

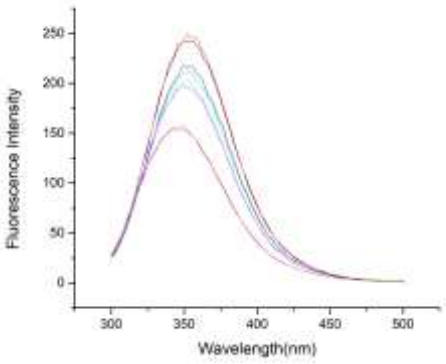

(б)

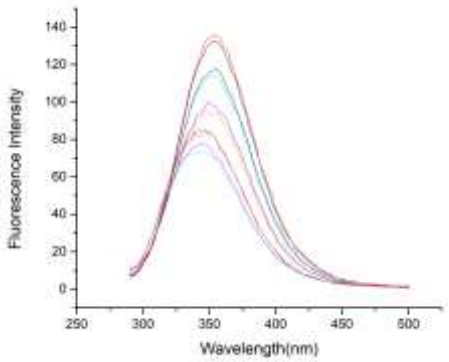

(в)

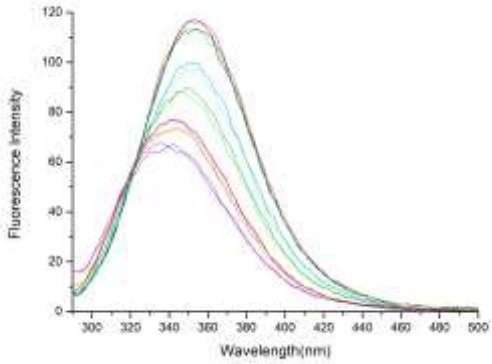

(г)

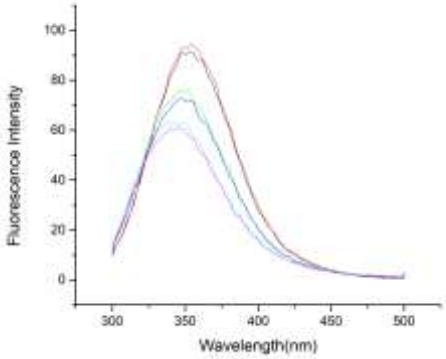

(д)

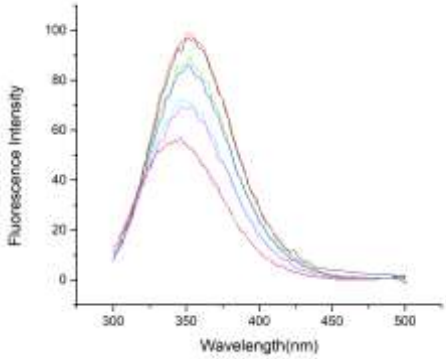

(е)

*e-mail: proletina.kardaleva@orgchm.bas.bg

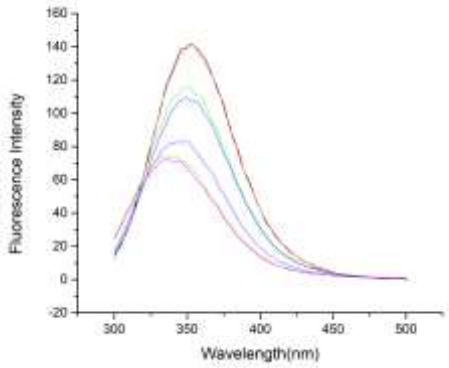

(ж)

Фигура 2. Емисионни спектри на комплексите на BSA с IBU (а), [L-ValOEt][IBU] (б), [L-LeuOEt][IBU] (в), [L-ValOPr][IBU] (г), [L-LeuOPr][IBU] (д), [L-ValOiPr][IBU] (е), [L-ValOBu][IBU] (ж). Концентрацията на BSA е 2μM, а на лигандите от 0,5 μM до 0,1 mM.

В емисионните спектъри на албумина в присъствие на ЙТ с анион ибупрофен се наблюдава хипсохромно отместване на максимума, което е индикация за това, че обкръжението в близост до флуорофорите става по-полярно. Ефектът е концентрационно зависим и е индикация за конформационна промяна.

Напроксенът и неговите производни се характеризират с емисионен максимум припокриващ се с този на албумина и флуоресценцията не може да се използва като индикация за образуване на техните комплекси и/или да се проследят промени в третичната структура на протеина.

За да установим на ефекта на ЙТ с аниони напроксен и ибупрофен върху вторичната структура на албумин използвахме инфрачервена спектроскопия. Ние проследихме промените в интензивността и профила на Амид I ивицата (1700– 1600 cm^{-1}) на албумин в присъствие на ЙТ. Тази ивица е много чувствителна към промени в геометрията и обкръжението на амидните групи от полипептидната верига.

На фигура 3 за илюстрация е показан оригиналният спектър (А), втората производна (Б) и деконволюираният („разложен“) спектър на нативен BSA във фосфатен буфер (В). По аналогичен начин са обработени всички спектри на комплекси на албумин и ЙТ, съдържащи аниони ибупрофен и напроксен. Определени са площите и съответно дела на структурните елементи за всяка от получените ивици, изграждащи Амид I ивицата и според позицията на максимумите им са отнесени към определена вторична структура според приетата литература.

*e-mail: proletina.kardaleva@orgchm.bas.bg

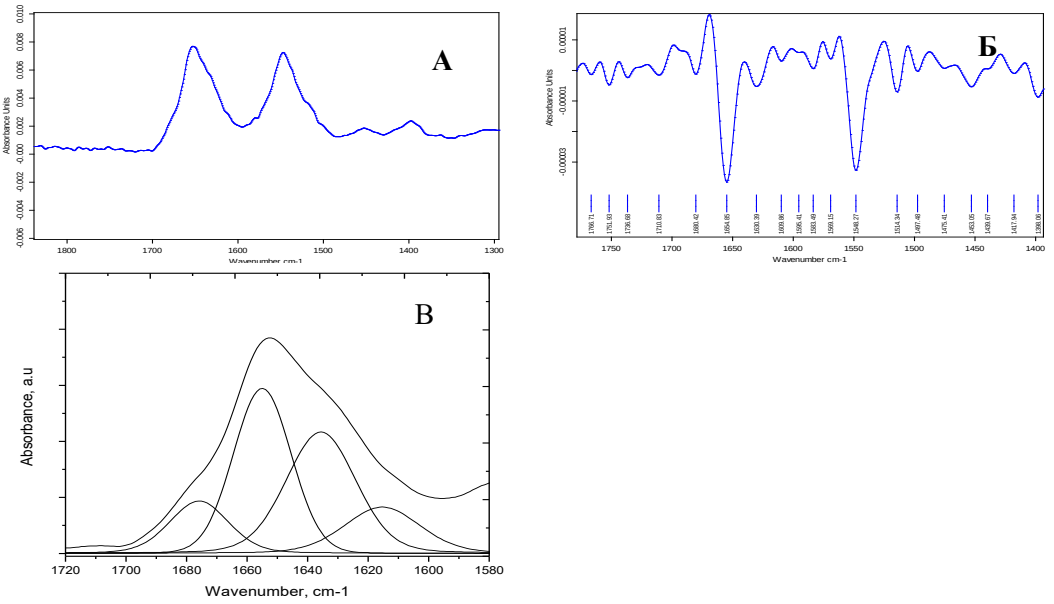

Фигура 3. Оригиналнен ИЧ спектър (А), втора производна (Б) и разложен ИЧ спектър (В) на BSA в областта 1700-1400 см$^{-1}$.

Обобщените резултати са показани в таблица 3 и таблица 4 за сериите ЙТ, съдържащи аниони напроксен и ибупрофен.

Таблица 3. Компоненти на Амид I ивицата за комплексите на BSA с ЙТ с анион напроксен(1:1).

Комплекс	α- спирали		β-структури		ароматни остатъци / агрегирали структури / антипаралелни β-листове	
	Позиция (cm^{-1})	Площ (%)	Позиция (cm^{-1})	Площ (%)	Позиция (cm^{-1})	Площ (%)
Нативен BSA	1656	26,5	1636 1673	48,1 7,0	1615	18,4
BSA-NAP	1655	27,9	1625 1640 1669 1681	17,0 25,0 11,4 4,5	1610 1696	11,8 2,3
BSA-[L-ValOEt][NAP]	1657	28,3	1628 1644 1675	18,3 23,4 17,3	1612 1700	12,0 0,6
BSA-[L-ValOPr][NAP]	1655	25,4	1625 1640 1673	24,1 21,6 14,6	1606 1697	13,4 0,8
BSA-[L-ValOiPr][NAP]	1654	41,4	1633 1678	30,6 0,9	1615 1684	13,8 13,7
BSA-[L-LeuOEt][NAP]	1654	33,6	1620 1636 1674	14,1 26,0 15,2	1601 1697	8.7 2,5

*e-mail: proletina.kardaleva@orgchm.bas.bg

Таблица 4. Компоненти на Амид I ивицата за комплексите на BSA с ЙТ с анион ибупрофен (1:1).

	α- спирали		β-структури		неподредени структури		ароматни остатъци / агрегирали структури / антипаралелни β-листове	
	Позиция на ивица-та (cm^{-1})	Относителна площ (%)	Позиция на ивица-та (cm^{-1})	Относителна площ (%)	Позиция на ивицата (cm^{-1})	Относителна площ (%)	Позиция на ивицата (cm^{-1})	Относитена площ (%)
Нативен BSA	1656	26,5	1636 1673	48,1 7,0	-	-	1615	18,4
BSA-IBU	1657	30,2	1626 1643 1675	9,6 41,8 13,2	-	-	1616	5,3
BSA-[L-ValOEt][IBU]	1657	37,6	1636 1674	22,4 20,6	1649	19,3	-	-
BSA-[L-LeuOEt][IBU]	1657	35,0	1628 1643 1673	14,5 29,2 11,3	-	-	1614	10,1
BSA-[L-ValOPr][IBU]	1655	18,6	1640 1670	75,7 5,7	-	-	-	-
BSA-[L-LeuOPr][IBU]	1657	31,1	1627 1638 1672	12,6 14,8 15,2	1649	18,1	1616	8,1
BSA-[L-ValOiPr][IBU]	1655	37,3	1636 1675	36,6 11,8	-	-	1612	14,3
BSA-[L-ValOBu][IBU]	1658	28,5	1632 1647 1674	25,7 23,3 12,7	-	-	1619	9,9

Очаквано, свързването на лигандите в някой от свързващите подцентрове на албумина индуциира неговата конформационна промяна. За серията ЙТ с анион напроксен, установихме, че в присъствие на [L-ValOiPr]-производното молекулата на албумина е по-подредена, нараства дела на α-спиралите за сметка на β-структурите, но също така и на агрегатите. При останалите ЙТ от тази серия се наблюдава преструктуриране на молекулата на албумина, но се запазва свързващия капацитет. Серията ЙТ с анион ибупрофен предизвикват по-значими промени в конформацията на албумина. Резултатът е в съгласие с наблюдаваните по-ниски константи на свързване с тази серия съединения. Интересно е да се отбележи, че в присъствие на [L-ValOPr][IBU] албуминът е почти напълно денатуриран. Вижда се, че β- структурите са над 80%, но не се наблюдава образуването на агрегати. В присъствието на [L-ValOEt][IBU] и [L-LeuOPr][IBU] нараства дела на неподредените структури, което е възможно обеснение за

*e-mail: proletina.kardaleva@orgchm.bas.bg

по-ниската ефективност на свързване.

Изследвахме ефекта на ЙТ с анион напроксен върху термодинамичната стабилност на албумин. На фигура 4 е показан профила на денатурираните кривите при диференциална сканираща калориметрия.

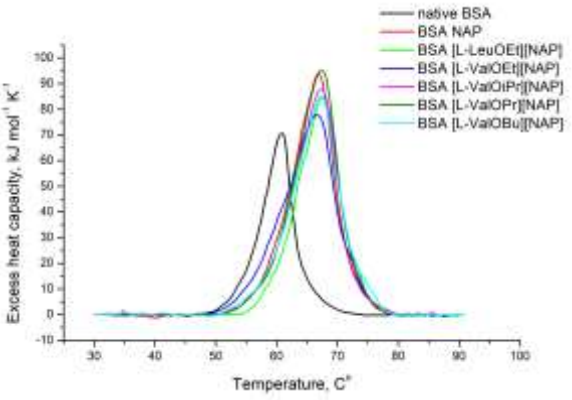

Фигура 4. Крива на диференциална сканираща калориметрия на BSA в присъствие на ЙТ, съдържащи анион напроксен. Съотношението: протеин: ЙТ е 1:1.

Както се вижда от термограмите, албуминът е по-термостабилен в присъствие на ЙТ с анион напроксен. Резултатите са в съгласие с наблюдаваните конформационни промени. Експерименталното деконволюиране позволява да се различат три термодинамични прехода, които вероятно се дължат на сравнително независимо температурно-разгъване на трите ясно обособени структурни домена (таблица 5).

Таблица 5. Термодинамични параметри, получени чрез експериментално деконволюиране на термограмите при диференциална сканираща калориметрия за нативния BSA и неговите комплекси с ЙТ на напроксена, получени в съотношение 1:1.

	T_{m1}/°C	ΔH_1/kJ mol^{-1}	T_{m2}/°C	ΔH_2/kJ mol^{-1}	T_{m3}/°C	ΔH_3/kJ mol^{-1}	ΔH_{total}/kJ mol^{-1}
Нативен BSA	57	128	60,6	253,9	63,1	119	492,2
BSA-NAP	62,5	269,2	67,3	470,2	71,8	93,1	849,8
BSA-[L-LeuOEt][NAP]	64,5	263,7	68	324,7	71,2	135,6	759
BSA-[L-ValOEt][NAP]	61,8	341,8	66,6	365,3	70,9	118,8	846
BSA-[L-ValOiPr][NAP]	63,2	334,7	67,4	307,9	69,9	187,9	836
BSA-[L-ValOPr][NAP]	63,9	425,5	67,6	248,5	70	199,2	882,8
BSA-[L-ValOBu][NAP]	63,2	342,7	67,2	366,6	70,1	170,6	860

*e-mail: proletina.kardaleva@orgchm.bas.bg

Към момента се провеждат диференциална сканираща калориметрия експерименти за установяване на температурната стабилност на албумин в присъствие на ЙТ с анион ибупрофен и предстои резултатите да бъдат обобщени.

Изводи/Обобщение

Като цяло изследваните ЙТ с аниони ибупрофен и напроксен и катиони алкилови естери на аминокиселини се характеризират с параметри на свързване към албумин близки до тези на изходните ибупрофен и напроксен. Разликите в конформацията на албумина в присъствие на изследваните ЙТ вероятно се дължат на свързването им към различни подсвързващи центрове. Най-общо изследваните ЙТ не стимулират агрегацията на протеина. ЙТ с аниони напроксен повишават термодинамичната стабилност на албумина. Очакваме ЙТ на основата на ибупрофен да имат подобен ефект.

Резултатите може да са основа за предлагане на модификации в катиона и получаване на нови ЙТ, които да са с подобрени параметри на свързване, съответно факмакокинетика и фармакодинамика.

Публикации и участия на научни форуми

Публикация, излязла от печат през втория отчетен период

Ossowicz, P., Janus, E., Klebeko, J., Świątek, E., Kardaleva, P., Taneva, S., Krachmarova, E., Rangelov, M., Todorova, N. and Guncheva, M. „Modulation of the binding affinity of naproxen to bovine serum albumin by conversion of the drug into amino acid ester salts.“ *Journal of Molecular Liquids,* 2020, *319*, 114283; https://doi.org/10.1016/j.molliq.2020.114283

Участия на научни форуми през втория отчетен период

1. Тринадесети пролетен семинар-уебинар “Интердисциплинарна химия“, 22-24 юни 2020г., гр.София;
Организатор: Институт по оптически материали и технологии БАН
Устен доклад: „Ефект от превръщането на напроксена в йонни течности върху свързването им с говежди серумен албумин“
Автори: Пролетина Кардалева, Мая Гунчева

2. Scientific Conference: Research Infrastructure in support of Science, Technology and Culture Sofia, September, 29-30, 2020- On-line meeting;
Организатор: Inframat
Постерен доклад: „Study of the Conformation and Thermal Stability of Bovine Serum Albumin in Complexes with Ionic Liquids Containing Naproxen Anion“
Автори: P. Kardaleva, S. Todinova, D. Yancheva, M. Guncheva

Дата: 04.02.2021 г. Изготвил: …….
/П.Кардалева/

*e-mail: proletina.kardaleva@orgchm.bas.bg

Journal of Molecular Liquids 319 (2020) 114283

Contents lists available at ScienceDirect

Journal of Molecular Liquids

journal homepage: www.elsevier.com/locate/molliq

Modulation of the binding affinity of naproxen to bovine serum albumin by conversion of the drug into amino acid ester salts

Paula Ossowicz [a], Ewa Janus [a], Joanna Klebeko [a], Ewelina Światek [a], Proletina Kardaleva [b], Stefka Taneva [c], Elena Krachmarova [d], Miroslav Rangelov [b], Nadezhda Todorova [e], Maya Guncheva [b,*]

[a] West Pomeranian University of Technology, Faculty of Chemical Technology and Engineering, Department of Chemical Organic Technology and Polymeric Materials, Piastów Ave. 42, 71-065 Szczecin, Poland
[b] Institute of Organic Chemistry with Centre of Phytochemistry, Bulgarian Academy of Sciences, Acad. G. Bonchev Bl. 9, 1113 Sofia, Bulgaria
[c] Institute of Biophysics and Biomedical Engineering, Bulgarian Academy of Sciences, Acad. G. Bonchev Str. 21, 1113 Sofia, Bulgaria
[d] Institute of Molecular Biology "Roumen Tsanev", Bulgarian Academy of Sciences, Acad. G. Bonchev Str, Block 21, 1113 Sofia, Bulgaria
[e] Institute of Biodiversity and Ecosystem Research, Bulgarian Academy of Sciences, 2 Yuri Gagarin Street, 1113 Sofia, Bulgaria

ARTICLE INFO

Article history:
Received 3 August 2020
Received in revised form 2 September 2020
Accepted 8 September 2020
Available online 14 September 2020

Keywords:
Ionic liquids
Albumin
Binding affinity
Naproxen derivatives
Isothermal titration calorimetry
Molecular docking

ABSTRACT

Naproxen (NAP) is one of the most widely prescribed non-steroidal anti-inflammatory drugs. Novel formulations of NAP aiming at better water-solubility, dosage, and the onset of action or new routes of application in order to minimize or prevent side effects of NAP are in the current interest of the pharmaceutical industry. Here, we report the synthesis, chemical, spectral and physicochemical characterization of a series of salts containing cations amino acid alkyl esters (AAE) and NAP anion, which potentially can be used as novel drug formulation. The [L-AAE][NAP] were obtained in three steps: preparation of the AAE hydrochlorides, neutralization of the hydrochlorides to the corresponding AAE, and formation of the target organic salts. All NAP derivatives, tested at a concentration as high as 100 μM, exhibited no toxicity against murine macrophage cell line (RAW 264.7). The binding parameters and stoichiometry of [AAE][NAP]s to bovine serum albumin (BSA) are in the range of that estimated for the parent NAP. Only L-valine isopropyl ester naproxenate characterizes with about one order of magnitude lower binding affinity for BSA, which suggests a faster diffusion rate in the circulatory system than the parent NAP and other derivatives, and therefore faster reach to the target system. Using molecular modeling seven binding pockets of BSA were probed for their suitability to binds the cation and the anion and results are discussed in correlation with the obtained thermodynamic parameters for the binding of NAP derivatives to BSA.

1. Introduction

Ionic liquids (ILs) are organic salts, typically composed of bulky organic cations and organic or inorganic anions [1]. Their physicochemical properties are tunable and can be easily modulated by an appropriate selection or modification of the cation and the anion. In recent years, ILs have demonstrated significant potential in pharmaceutical research and development [1]. Some ILs are applied as catalysts, solvents or co-solvents in the synthesis of active pharmaceutical ingredients (API) or their precursors, which in some cases offers the advantages of increased reaction rate, enhanced enantioselectivity, higher purity and/or yields of the target products, or may facilitate the isolation of the target product [2–4]. ILs can be used in the processes of separation and purification of APIs as well as the removal of APIs from wastewater [5]. It is noteworthy to be mentioned that many ILs exhibit biological activities such as anti-bacterial, anti-fungal, anti-cancer, *etc.* and have the potential for biomedical applications [6].

ILs and organic salts have also been successfully applied in the preparation of novel drug delivery systems *e.g.* Sidat et al. developed new IL-oil microemulsions for transdermal delivery of acyclovir [7]. On the other hand, the conversion of hydrophobic drugs into ILs or organic salts using suitable counter ions may solve problems with their low solubility in aqueous media and therefore to enhance their bioavailability and possibly lowering the dosage and toxicity of the drug. For example, the water solubility of methotrexate was improved up to 5000 times by its conversion to choline-, trimethylammonium-, tributylphosphonium- or amino acid ester based-IL, while indomethacin-based ILs containing tetramethylguanidine, 2-dimethylaminoethanol, 1,8-diazabicyclo[5.4.0]undec-7-ene or 1,4-diazabicyclo[2.2.2]octane cation proved to be up to 700,000 times more water-soluble than the parent drug molecule [8,9]. Interestingly, enhanced blood-barrier permeation was reported for ILs containing donepezil (a drug for the treatment of Alzheimer's disease) cation and docusate, ibuprofenate, or free fatty acid anions [10,11].

* Corresponding author.
E-mail address: maiag@orgchm.bas.bg (M. Guncheva).

https://doi.org/10.1016/j.molliq.2020.114283
0167-7322/

Using relevant ions may result in novel formulation with a new route of administration. For example, Sahbaz et al. improved the oral drug exposure of itraconazole, cinnarizine, and halofantrine by their conversion into lipophilic ionic liquids, which facilitated subsequently their incorporation in the drug into lipid-based formulations and integration into lipid absorption pathways [12]. On the other hand, Park and Prausnitz proposed a fast method for delivery of lidocaine to skin based on a formulation containing lidocaine cation and ibuprofen anion, the novel formulation characterizes with increased sorption of the lidocaine into the skin and the local anesthesia occurs five times faster than a commercial topical formulation of lidocaine and prilocaine prepared as a eutectic mixture [13]. Tested *in vitro*, ILs based on 1,4-diazabicyclo[2.2.2]octanium, N,N-dialkylmorpholinium, and 1,3-dialkylimidazolium cations showed good potential as enhancers for transdermal permeation of diltiazem, a calcium channel blocker, and the formulations were less toxicity than traditional cationic surfactants [14].

The dual-functional API-ILs, which allow in one formulation to be combined two or more active compounds for simultaneous release are very attractive for the pharmaceutical industry. During the last decade, many dual-functional ILs, in which the ions exhibit either two independent pharmacological activities or have a synergetic mode of action were synthesized and *in vitro* tested [15–17].

Non-steroidal anti-inflammatory drugs (NSAIDs) are one of the most widely prescribed classes of medications, highly effective for the treatment of chronic and acute pain and inflammation [18]. Among other serious side effects, the prolonged use of NSAIDs may increase the risk of gastrointestinal incidents such as gastroduodenal ulcers, gastrointestinal bleeding, and perforation, dyspepsia, *etc.* [18]. One of the approaches to minimize or prevent such injuries is to decrease the toxicity of the NSAIDs *via* their distribution in alternative formulations such as enteric-coated or soluble preparations, which reduce the gastric residence and mucosal contact time [19]. Other approaches are the application of NSAIDs as buffered preparations or non-acidic pro-drugs, as well as other routes of administration of the drugs *e.g.* rectal, parental, topical, *etc.* [19]. In the recent years, ILs based on ketoprofen, naproxen, and ibuprofen, the most widely prescribed propionic acid-derived NSAIDs, have been in the focus of scientists in an attempt to optimize their solubility, dosage, duration, and the onset of action, parameters that may influence the gastrointestinal side effects. It is noteworthy to be mentioned that some promising results have been obtained. For example, ILs containing cholinium cation and naproxenate, ketoprofenate or ibuprofenate anion characterize with enhanced water solubility in comparison to the parent molecule or its sodium salt [20,21]. An enhanced water solubility without a negative effect on cytotoxicity on fibroblasts was reported for numerous ibuprofenate-based ILs containing 1,3-substituted imidazolium or substituted quaternary ammonium cations [21]. Interestingly, N-ethyl-N-(2-hydroxypropyl)-*N*,*N*-dimethylammonium ibuprofenate showed a relatively good selectivity and produced a strong antiproliferative effect on human ovarium carcinoma cells (A2780) with the estimated activity ratio above 13 for A2780 *versus* normal human dermal fibroblasts [21]. Recently, ibuprofen-based ILs with transdermal permeability and potential for a topical application have been synthesized and *in vitro* tested. For example, Moshikur et al. reported that in comparison to sodium ibuprofenate, *N*-methyl-pyrrolidonium ibuprofenate characterizes with an enhanced skin penetration and enriched drug circulation in the target tissue and lower cytotoxicity on murine fibroblasts (NIH3T3 and L929) and human liver cancer cells (HepG2) [22]. Expectedly, the substitution of the sodium cation of sodium ibuprofenate with L-valine ethyl esters, 1-butyl-3-methyl-imidazolium, procainium, ranitidinium, lidocainium, tetraalkylphosphonium or tetraalkylammonium led to increased skin permeability of the drug and can be used in the development of new topical medications [10,23]. Moreover, Wu et al. showed that 1-(2-hydroxyethyl)-3-methyl-imidazolium ibuprofenate and 1-butyl-3-methyl-imidazolium ibuprofenate are less toxic to keratinocytes (HaCat cells) than ibuprofen and its sodium salt [10]. Zhang et al. proposed a microemulsion containing lidocaine ibuprofenate as an oil phase as a promising vehicle for skin delivery of artemisinin, a poor soluble antimalarial drug [24]. Parra-Ruiz et al. synthesized wound dressing based on double-polymerizable salts containing cation quaternary ammonium with an antibacterial activity and anion NSAIDs (meclofenamic acid, ketoprofen or ibuprofen) with an anti-inflammatory activity, which could be applied for prolonged use – 10 days [25]. There are some other communications on the synthesis, physicochemical characterization, *in vitro*, and *in vivo* testing of ILs based on NSAIDs, however, their interactions with plasma proteins including serum albumin are scarcely studied [26,27].

Serum albumin is the most abundant plasma protein in vertebrates, which is responsible for the maintaining of the oncolytic pressure and the transport of hormones, fatty acids, drugs, metabolites, *etc.* in mammalians [28,29]. Bovine serum albumin (BSA) shows about 80% homology and high structural identity with human serum albumin, and due to the availability of extensive structural information, it is used in binding studies [29]. Moreover, BSA is used as a stabilizer and/or drug carrier for some drug formulations [30]. Human and bovine serum albumins are composed of three homologous domains (I-III), each subdivided into two subdomains (A and B) [28]. So-called Sudlow's site I (subdomain II A), site II (subdomain II A), and site III (subdomain I B) typically bind drugs, but there are also nine binding sites for free fatty acids, 4-hydroxine binding site (subdomain III B), metal binding site, heme-binding site, a site centered around Cys 34, N-terminal binding site, and some other [31,32]. The binding of drugs to serum albumin affects their pharmacokinetics and pharmacodynamics and is correlates with their dosage, efficiency, toxicity, and/or side effects [29]. In addition, serum albumin increases the apparent solubility of hydrophobic drugs and therefore modulates its delivery to cells *in vivo* and *in vitro*.

Here, we report the synthesis and characterization of a series of salts containing cations amino acid esters (AAE) and naproxenate anion, which potentially can be used as novel drug formulation. L-type neutral amino acids are attractive for the development of prodrugs or novel salt formulations of poorly soluble and adsorbed therapeutic agents, which is due to their lower toxicity and ability to cross the cell membrane including the blood-brain barrier *via* the corresponding transmembrane receptors [33]. The aim of the study is to investigate the effect of the conversion of the naproxen into AAE salts on their binding interactions with BSA using an experimental and theoretical approach. The toxicity of the compounds was tested toward the murine macrophage cell line (RAW 264.7).

2. Materials and methods

2.1. Materials

Naproxen was isolated from commercially available medicine Naproxen 500 Hasco® (dose of the active substance: 500 mg) (HASCO-LEK S.A. Wrocław, Poland). The extraction and purity determination were performed in accordance with the procedure described in Pharmacopeia. The compound was identified by NMR and elemental analysis.

All other reagents and solvents were commercially available materials and were used without further purification. L-Valine and L-Leucine (≥99.0%) were provided by Carl Roth (Karlsruhe, Germany). Trimethylsilyl chloride (TMSCl) (≥99%) was purchased from Sigma-Aldrich (Steinheim am Albuch, Germany). Ammonium hydroxide solution 25% ($NH_3{\cdot}H_2O$) was of analytical grade obtained from StanLab (Lublin, Poland). Ethanol (EtOH), propan-2-ol (i-PrOH), propan-1-ol (PrOH), butan-1-ol (BuOH), dimethyl sulfoxide, chloroform, ethyl acetate, diethyl ether, toluene and n-hexane of high purity were purchased from Chempur (Gliwice, Poland). Deuterated chloroform ($CDCl_3$) (99.8%) (+0.03% TMSCl) was provided by Eurisotop (Cheshire, England).

Murine monocyte macrophage cells (RAW 264.7) were obtained from American Type Culture Collection (ATCC, Manassas).

Bovine serum albumin (heat shock fraction, protease-free, free fatty acids free, essentially globulin free), Dulbecco's Modified Eagle's

Medium (DMEM) high glucose medium containing L-glutamine, antibiotic-antimycotic solution (100×) containing 10,000 units penicillin, 10 mg streptomycin and 25 μg amphotericin B per mL, dimethyl sulfoxide (DMSO) were purchased from Sigma-Aldrich. AlamarBlue™ cell viability reagent was purchased from ThermoFisher Scientific.

2.2. Synthesis of the L-amino acid ester naproxenates [L-AAOR][NAP]

The compounds were obtained using the modified, previously described method, in three steps (Scheme 1) [27]. In the first step, a suspension of amino acid in alkyl alcohol (ROH) was added to two molar equivalents of TMSCl. The reaction mixture was stirred vigorously overnight at room temperature. Then, the excess of TMSCl and the alcohol, and the formed by-products were removed by evaporation at 60 °C under vacuum. The product was purified from the residue of unreacted TMSCl and secondary TMSOH or TMSR formed, by washing with diethyl ether. The obtained product was then dissolved in chloroform and filtered under reduced pressure to withdraw the unreacted amino acid. The filtrate was distilled off under reduced pressure (60 °C, 10 mbar). The obtained hydrochloride was dried in a vacuum dryer at 60 °C and the pressure of 5 mbar, for 24 h. As a result, the amino acid alkyl ester hydrochlorides (L-AAOR·HCl) were obtained with good yield. In the second step, amino acid alkyl ester hydrochlorides were neutralized by the addition of one to three molar equivalents of 25% aqueous solution of ammonium hydroxide, and then the products were extracted with diethyl ether. The organic layer was separated and dried over anhydrous Na_2SO_4, then evaporated to obtain the corresponding amino acid alkyl esters [L-AAOR]. In the third step, the equimolar amount of the corresponding L-AAOR and naproxen were dissolved in chloroform. The solution was stirred thoroughly at room temperature for 20 min. Then, the solvent was evaporated under vacuum at 35 °C. The obtained naproxen derivatives were dried in a vacuum oven at 60 °C for 24 h. The synthesized [L-AAOR][NAP] in the form of white solids were identified using spectroscopic methods, *i.e.* ^{1}H, ^{13}C NMR, and FTIR spectroscopy. All NMR and FTIR spectra, TG and DSC curves for [L-AAOR][NAP] are available in the Supplementary.

2.3. Characterization of the L-amino acid ester naproxenates

The ^{1}H NMR and ^{13}C NMR spectra were recorded in $CDCl_3$ on a Bruker DPX-400 Avance III HD (Billerica, MA, USA) spectrometer operating at 400.13 MHz (^{1}H) and 100.62 MHz (^{13}C). The chemical shifts were referred to tetramethylsilane (TMS) as the internal standard.

The attenuated total reflectance Fourier transform infrared spectra (ATR-FTIR) were recorded on the FTIR spectrometer model Thermo Fisher Scientific 'Nicolet 380' (Waltham, MA, USA) equipped with a diamond ATR in transmission mode from 4000 to 400 cm^{-1} at a resolution of 4 cm^{-1}.

The UV–Vis absorption spectra were recorded in the wavelength range of 190–400 nm with an accuracy of ±1 nm using Spectroquant® Pharo 300 Spectrophotometer (Merck, Darmstadt, Germany) at 25 °C in a 10 mm quartz cell. The compounds were dissolved in absolute ethanol in a concentration range of 10^{-4}–10^{-5} M.

The elemental analysis was carried out on Thermo Scientific™ FLASH 2000 CHNS/O Elemental Analyzer (Waltham, MA, USA). The samples of 2–3 mg (CHNS analysis mode) and 1–2 mg (O analysis mode) were weighted with an accuracy of ±0.000001 g.

Thermogravimetric analysis was performed using thermomicrobalance TG 209 F1 Libra® from NETZSCH (Selb, Germany). Sample between 5 and 10 mg was placed in Al_2O_3 crucible. Measurements were carried out in an air atmosphere. The flow rate of air was 25 cm^3 min^{-1}, nitrogen flow 10 cm^3 min^{-1}. Nitrogen was used as a protective gas.

The specific rotation $[\alpha]_D^{20}$ was registered using AUTOPOL IV Polarimeter from Rudolph Research Analytical (Hackettstown, NJ, USA). The measurements were collected at 20 °C for solutions with a concentration of 0.01 g cm^{-3}. Ethanol was used as the solvent.

The melting point was measured using MPA100 Melting Point Apparatus with an automated melting point system from SRS – Stanford Research Systems. Measurements were carried out within the temperature range of 25 °C to 400 °C. The heating rate was 2 °C min^{-1}, measurement accuracy was 0.3 °C.

The solubility of naproxen and its derivatives was evaluated in polar and nonpolar solvents by modified Vogel's method at the temperature of 25 °C [34]. By this method, the compound was classified as soluble, partially soluble, and insoluble. Dimethyl sulfoxide, ethanol, chloroform, ethyl acetate, diethyl ether, toluene, an d n-hexane were used as solvents.

2.3.1. L-leucine ethyl ester naproxenate [L-LeuOEt][NAP]

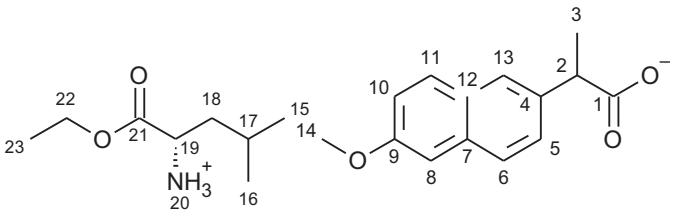

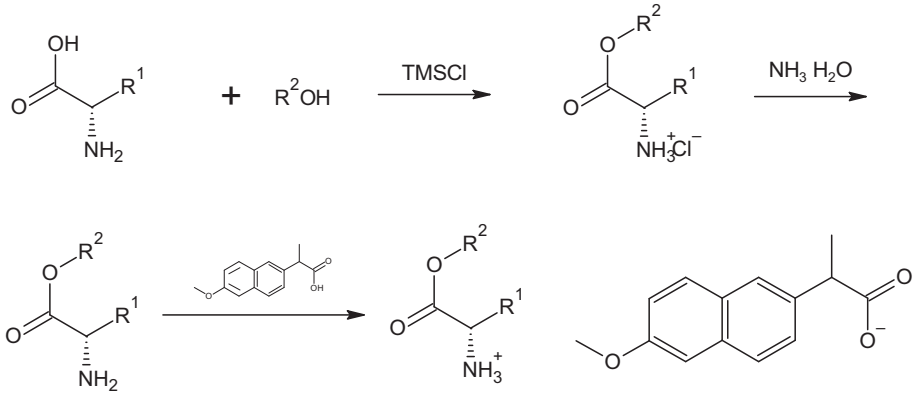

Scheme 1. The general synthetic path for [L-AAOR][NAP].

UV–Vis (EtOH): λ_{max} = 228.0 nm; $\mathbf{T_m}$ = 129.1–132.4 °C; $[\alpha]_D^{20}$ = +29.052 (c = 0.519 g/100 cm^3 EtOH).

^{1}H NMR (400 MHz, $CDCl_3$) δ in ppm: 7.57–7.54 (s + d, 3H, H6, H8, H11); 7.33 (d, $J_{10,11}$ = 8.5 Hz, 1H, H10); 7.03–6.98 (s + d, 2H, H5, H13); 6.21 (s, 3H, H20); 4.07–3.99 (m, 2H, H22); 3.81 (s, 3H, H14); 3.71–3.66 (dd, 1H, H2); 3.44–3.41 (dd, 1H, H19); 1.64–1.54 (m, 1H, H18); 1.47–1.40 (m, 4H, H3, H17); 1.37–1.29 (m, 1H, H18); 1.13 (t, $J_{23,22}$ = 7.1 Hz, 3H, H23); 0.76 (t, $J_{15(16),17}$ = 7.8 Hz, 6H, H15, H16).

^{13}C NMR (100 MHz, $CDCl_3$) δ in ppm: 179.11 (C1); 174.79 (C21); 157.45 (C9); 136.64 (C4); 133.56 (C7); 129.28 (C11); 128.96 (C12); 126.94 (C6); 126.53 (C13); 125.92 (C5); 118.74 (C10); 105.55 (C8); 61.23 (C22); 55.28 (C14); 52.03 (C19); 46.15 (C2); 42.85 (C18); 24.60 (C17); 22.69 (C16); 21.82 (C15); 18.61 (C3); 14.12 (C23).

Elemental analysis: Calc. (%) for $C_{22}H_{31}NO_5$ (389.485 g/mol) C (67.84), H (8.02), N (3.60), O (20.54). Found C (67.86), H (7.99), N (3.61), O (20.55).

2.3.2. L-valine ethyl ester naproxenate [L-ValOEt][NAP]

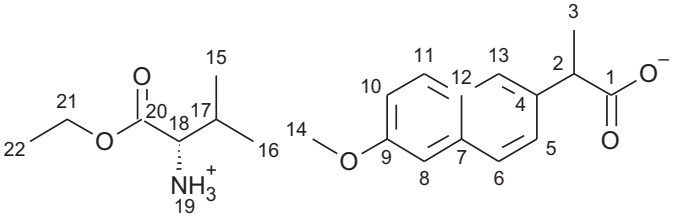

UV–Vis (EtOH): λ_{max} = 228.0 nm; $\mathbf{T_m}$ = 131.8–133.6 °C; $[\alpha]_D^{20}$ = + 29.630 (c = 0.502 g/100 cm^3 EtOH).

^{1}H NMR (400 MHz, $CDCl_3$) δ in ppm: 7.64 (s + d, 3H, H6, H8, H11); 7.40 (d, $J_{10,11}$ = 6.9 Hz, 1H, H10); 7.13–7.04 (s + d, 2H, H5, H13); 6.18 (s, 3H, H19); 4.13–4.01 (m, 2H, H21); 3.89 (s, 3H, H14); 3.83–3.73 (dd, 1H, H); 3.36 (d, $J_{18,17}$ = 4.6 Hz, 1H, H18); 2.13–1.91 (m, 1H, H17); 1.52 (d, $J_{3,2}$ = 7.1 Hz, 3H, H3); 1.21 (t, $J_{22,21}$ = 7.2 Hz, 3H, H22); 0.98–0.75 (m, 6H, H15, H16).

^{13}C NMR (100 MHz, $CDCl_3$) δ in ppm: 179.20 (C1); 173.63 (C20); 157.48 (C9); 136.42 (C4); 133.59 (C7); 129.27 (C13); 128.95 (C12); 126.97 (C6); 126.49 (C13); 125.95 (C5); 118.77 (C10); 105.56 (C8); 61.07 (C21); 58.95 (C18); 55.27 (C14); 46.01 (C2); 31.41 (C17); 18.69 (C16); 18.53 (C15); 17.28 (C14); 14.18 (C22).

Elemental analysis: Calc. (%) for $C_{21}H_{29}NO_5$ (375.464 g/mol) C (67.18), H (7.79), N (3.73), O (21.31). Found C (67.10), H (7.78), N (3.74), O (20.94).

2.3.3. L-valine propyl ester naproxenate [L-ValOPr][NAP]

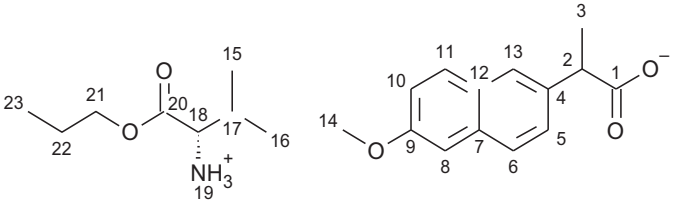

UV–Vis (EtOH): λ_{max} = 229.0 nm; $\mathbf{T_m}$ = 116.2–118.2 °C; $[\alpha]_D^{20}$ = + 31.034 (c = 0.522 g/100 cm^3 EtOH).

^{1}H NMR (400 MHz, $CDCl_3$) δ in ppm: 7.72–7.62 (s + d, 3H, H6, H8, H11); 7.45 (d, $J_{10,11}$ = 8.5 Hz, H10); 7.14–7.06 (s + d, 2H, H13, H5); 5.33 (s, 3H, H19); 4.12–3.97 (m, 2H, H21); 3.90 (s, 3H, H14); 3.85–3.75 (m, 1H, H2); 3.38 (d, $J_{18,17}$ = 4.6 Hz, 1H, H18); 2.11–1.98 (m, 1H, H17); 1.69–1.58 (m, 2H, H22); 1.54 (d, $J_{3,2}$ = 7.2 Hz, 3H, H3); 1.16–0.63 (m, 9H, H15, H16, H23).

^{13}C NMR (100 MHz, $CDCl_3$) δ in ppm: 179.09 (C1); 174.26 (C20); 157.53 (C9); 136.16 (C4); 133.64 (C7); 129.28 (C11); 128.95 (C12); 127.02 (C6); 126.43 (C13); 125.98 (C5). 118.82 (C10); 105.56 (C8); 66.65 (C21); 59.13 (C18); 55.28 (C14); 45.83 (C2); 31.60 (C17); 21.93 (C22); 18.85 (C16); 18.46 (C15); 17.24 (C3); 10.38 (C23).

Elemental analysis: Calc. (%) for $C_{22}H_{31}NO_5$ (389.491 g/mol) C (67.84), H (8.02), N (3.60), O (20.54). Found C (67.85), H (8.05), N (3.58), O (20.17).

2.3.4. L-valine isopropyl ester naproxenate [L-ValOiPr][NAP]

UV–Vis (EtOH): λ_{max} = 228.0 nm; $\mathbf{T_m}$ = 132.4–134.5 °C; $[\alpha]_D^{20}$ +30.740 (c = 0.527 g/100 cm^3 EtOH).

^{1}H NMR (400 MHz, $CDCl_3$) δ in ppm: 7.69–7.62 (s + d, 3H, H6, H8, H11); 7.41 (d, $J_{11,10}$ = 8.5 Hz, 1H, H10); 7.14–7.06 (s + d, 2H, H13, H5); 5.31 (s, 3H, H19); 5.09–4.95 (m, 1H, H17); 3.90 (s, 3H, H14); 3.84–3.74 (m, 1H, H2); 3.34 (d, $J_{18,17}$ = 4.6 Hz, 1H, H18); 2.10–1.97 (m, 1H, H17); 1.54 (d, $J_{3,2}$ = 7.2 Hz, 3H, H2); 1.22 (d, $J_{17,15}$ = 6.3 Hz, 6H, H15, H16); 0.92 (d, $J_{23,21}$ = 6.9 Hz, 3H, H22); 0.86 (d, $J_{22,21}$ = 6.9 Hz, 3H, H23).

^{13}C NMR (100 MHz, $CDCl_3$) δ in ppm: 179.10 (C1); 173.35 (C20); 157.46 (C9); 136.38 (C4); 133.59 (C7); 129.27 (C11); 128.94 (C12); 126.98 (C6); 126.48 (C13); 125.94 (C5); 118.77 (C10); 105.53 (C8); 68.71 (C21); 59.00 (C18); 55.27 (C14); 45.97 (C2); 31.45 (C17); 21.76 (C22/23); 18.73 (C16); 18.53 (C15); 17.20 (C3).

Elemental analysis: Calc. (%) for $C_{22}H_{31}NO_5$ (389.491 g/mol) C (67.84), H (8.02), N (3.60), O (20.54). Found C (67.46), H (8.05), N (3.59), O (20.16).

2.3.5. L-valine butyl ester naproxenate [L-ValOBu][NAP]

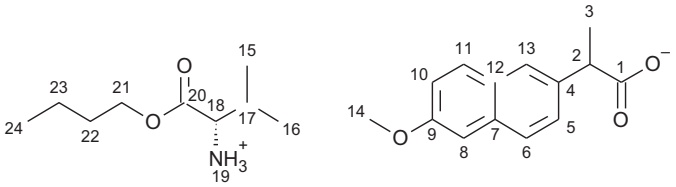

UV–Vis (EtOH): λ_{max} = 229.0 nm; $\mathbf{T_m}$ = 101.1–103.9 °C; $[\alpha]_D^{20}$ = + 29.750 (c = 0.521 g/100 cm^3 EtOH).

^{1}H NMR (400 MHz, $CDCl_3$) δ in ppm: 7.74–7.61 (s + d, 3H, H6, H8, H11); 7.41 (d, $J_{11,10}$ = 8.4 Hz, 1H, H11); 7.16–7.07 (s + d, 2H, H5, H13); 4.52 (s, 3H, H19); 4.18–4.03 (m, 2H, H21); 3.90 (s, 3H, H14); 3.87–3.77 (dd, 1H, H2); 3.36 (d, $J_{18,17}$ = 4.7 Hz, 1H, H18); 2.11–1.99 (m, 1H,17); 1.66–1.53 (d + m, 5H, H3, H22); 1.45–1.30 (m, 2H, H23); 0.98–0.85 (m, 9H, H15, H16, H23).

^{13}C NMR (100 MHz, $CDCl_3$) δ in ppm: 179.04 (C1); 174.53 (C20); 157.57 (C9); 135.90 (C4); 133.68 (C7); 129.29 (C11); 128.95 (C12); 127.08 (C6); 126.37 (C13); 126.01 (C5); 118.88 (C10); 105.58 (C8); 64.87 (C21); 59.26 (C18); 55.29 (C14); 45.65 (C2); 31.70 (C17); 30.61 (C22); 19.03 (C16); 18.41 (C15); 17.21 (C3); 13.65 (C24).

Elemental analysis: Calc. (%) for $C_{23}H_{33}NO_5$ (403.517 g/mol) C (68.46), H (8.24), N (3.47), O (19.825). Found C (68.67), H (8.27), N (3.48), O (19.34).

2.3.6. Naproxen [NAP]

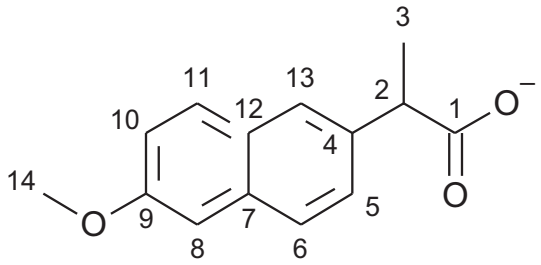

UV–Vis (EtOH): λ_{max} = 229.0 nm; $\mathbf{T_m}$ = 153.2–155.6 °C; $[\alpha]_D^{20}$ = + 50.988 (c = 0.514 g/100 cm^3 EtOH).

^{1}H NMR (400 MHz, $CDCl_3$) δ in ppm: 7.61–7.58 (s + d, 3H, H6, H8, H11); 7.31 (d, $J_{10,11}$ = 8.5 Hz, 1H, H10); 7.05–7.00 (s + d, 2H, H5, H13); 3.80–3.74 (m, 4H, H2, H14); 1.49 (d, $J_{2,3}$ = 7.2 Hz, 3H, H3).

^{13}C NMR (100 MHz, $CDCl_3$) δ in ppm: 181.00 (C1); 157.73 (C9); 134.92 (C4); 133.85 (C7); 129.36 (C11); 128.93 (C12); 127.28 (C6); 126.25 (C13); 126.20 (C5); 119.09 (C10); 105.62 (C8); 55.33 (C14); 45.35 (C2); 18.17 (C3).

Elemental analysis: Calc. (%) for $C_{14}H_{14}O_3$ (230.263 g/mol) C (73.03), H (6.13), O (20.85). Found C (73.85), H (6.17), N (0), O (20.44).

2.4. Cell culture

Murine macrophages RAW 264.7 were cultured in DMEM high glucose medium containing L-Glutamine, antibiotic mixture (with 10,000 units penicillin, 10 mg streptomycin, and 25 μg amphotericin B per mL) and 10% fetal bovine serum. The cells were cultivated at a humified atmosphere, 37 °C, and 5% CO_2.

For the experimental procedures, cells were seeded in a sterile 96-well plate at 8×10^4 cells per well and incubated for 48 h at 37 °C and 5% CO_2 for obtaining 70% confluency. Then, the cells were incubated for an additional 24 h with NAP or [AAOR][NAP] at concentrations 1, 10, and 100 μM. Control experiments with non-treated cells, treated with 1% DMSO (the solvent used to prepare the stock solution of the samples) and 100 μg NaF and 1% DMSO were performed.

2.5. Cell viability assay

The cell viability of RAW 264.7 cells in the presence of naproxen and its aminoacid salts was assessed in a colorimetric assay using an Alamar Blue reagent. The reagent was diluted with DMEM media (1:10), an aliquot of 10 μL of the solution was added to each well and incubated for 3 h at 37 °C underflow of 5% CO_2.

The measurements were carried out at an excitation wavelength of 544 nm and an emission wavelength of 590 nm with a 96-well plate reader FLUOstar Galaxy (Tecan BMG Labtechnologies). The survival of the cells, treated with different concentrations of the tested compounds, was presented in percentages from the control (non-treated cells).

The values are presented as mean ± standard deviation of three independent experiments. The values were considered to be significantly different if the p value was <0.05.

2.6. Isothermal titration calorimetry (ITC)

ITC experiments were carried out with a MicroCal ITC200 (MicroCal, Inc., Northampton, MA) with an operating cell volume of 300 μL. Stock solutions (10 nM) of NAP and [AAOR][NAP] were prepared in pure DMSO and were diluted in 20 mM phosphate saline buffer (PBS) (pH 7.4) to obtain the final working solution concentrations containing 1% DMSO. The protein solution (32 μM in 20 mM PBS (pH 7.4) containing 1% DMSO) was placed in the calorimeter cell and titrated by NAP and [AAOR][NAP] in 16 successive injections of 2 μL at 120 s interval, the first injection was of 1 μL and was not considered in the analysis of the isotherm. All experiments were performed at a fixed temperature of 298.15 K. All experiments were performed at a fixed temperature of 298.15 K with a constant stirring speed of 250 rpm. The heat of dilution of each ligand, NAP or [AAOR][NAP], titrated into buffer was used to correct the experimental data.

From the fit of the binding curves the binding constant Ka (Kd = 1/Ka) and the enthalpy ΔH° of the binding reaction were directly obtained. The Gibbs free energy of binding (ΔG°) and the entropy (ΔS°) are determined from the basic thermodynamic expression $\Delta G^\circ = -RTlnKa = \Delta H - T\Delta S^\circ$, where R and T are the gas constant and the absolute temperature, respectively. The reported data are mean ± S.D. values from three independent experiments.

2.7. Molecular modeling

In order to study the most probable binding sites of BSA with NAP and [AAOR][NAP] ligands, we made a hydrated and relaxed in physiological conditions BSA. In this study, the crystal structure of BSA [4f5s PDB code] was used and it was taken from RCSB Protein Data Bank [35]. The structure was checked for improperties, the found ones were corrected by Coot 0.9 [36] and protons were added in order to achieve the right protonated state of the structure at pH 7. The structure was relaxed by 100 ns molecular dynamics (MD) simulation. The MD simulations were done using the GROMACS software package. And the MD protocol consisted of force field parameterization with GROMACS program pdb2gmx, structure in vacuum energy minimization, solvent addition – GROMACS solvate program, Na^+ and Cl^- ions at 0.15 M concentration – GROMACS genion program, energy minimization, MD run position restrained of heavy solute atoms (PR run) and production MD run/s in NPT ensemble [37–46]. The temperature was kept constant at 37 °C by applying Berendsen and V-rescale thermostats during PR and production run, respectively. Berendsen barostat was used in equilibration MD runs and Parrinello-Rahman barostat – for production MD runs. Long-range electrostatic interactions were treated by applying the Particle Mesh Ewald algorithm [47] with a 1.2 nm cut-off radius for short-range interactions. Switch function was used for van der Waals interactions calculations with 1.2 nm cut-off radius and 1 nm switching distance. We used the Leap-frog integration algorithm with 2 fs time step as the covalent bonds connecting hydrogen atoms with the solute heavy atoms were kept with fixed length by the LINCS algorithm [48] and RATTLE algorithm [49]– used to keep the solvent molecules rigid. The last 50 ns from the production run were used for further analysis. Frames from a selected part of the trajectory were used for cluster analysis using RMSD (Root Mean Square Deviation of atomic position) between structures of BSA in a distance measurement in clustering. Two most populated clusters were selected and the frames most closely situated to the middle of these clusters in terms of RMSD were used for further docking study.

Ligands were protonated according to their protonation state at pH 7.4 and the conformation library for the docking study was generated using LowModeMD methodology with MMFF94 force field and energy window for collection of conformations 7 kcal/mol from the lowest energy conformation.

Docking was performed by the Molecular Operating Environment (MOE) software package.

To assess the most feasible binding pockets for NAP and the tested NAP-derivatives in BSA we collected possible pockets for our study by superposition of existing XDR structures of bovine serum albumin in complex with ligands. Then, for the future docking after aligning the albumin structures we selected the regions in which ligands are positioned. In Table 1 are given the selected according to this procedure seven most probable binding pockets (column 1). The numbering of the chain is according to the mature albumins [50,51]. In column 2 are shown the closest residues of albumin structure to the binding pocket

Table 1
Probable binding sites, amino acids comprising them, and name of the binding site according to the literature.

Probing binding site	Amino acids surrounding binding pocket	Pocket in literature
1	149TYR, 151PRO, 152GLU, 155TYR, 156TYR, 194ARG, 195GLN, **198ARG**, 210LEU, **213TRP**, 214SER, **217ARG**, **218LEU**, 219SER, **221LYS**, 222PHE, 229GLU, 230VAL, 231THR, 232LYS, **233LEU**, 234VAL, 235THR, 236ASP, 237LEU, 238THR, 239LYS, 240VAL, 241HIS, 244CYS, 252CYS, 253ALA, 254ASP, 255ASP, 256ARG, 257ALA, 258ASP, **259LEU**, 260ALA, 261LYS, 262TYR, **263ILE**, 264CYS, 270ILE, 274LEU, 277CYS, 282LEU, 283LEU, 284GLU, 285LYS, 286SER, 287HIS, 288CYS, **289ILE**, **290ALA**, 291GLU, 292VAL, 342VAL	Fatty acid 7 site [50, 51]
2	112LEU, 113PRO, 114LYS, **115LEU**, **116LYS**, 117PRO, 118ASP, 119PRO, 121THR, **122LEU**, **133PHE**, 136LYS, **137TYR**, **138LEU**, 139TYR, 140GLU, **141ILE**, 142ALA, 143ARG, 144ARG, 145HIS, 153LEU, 156TYR, **160TYR**, 163VAL, **164PHE**, 177LEU, 178LEU, 179PRO, 180LYS, **181ILE**, 182GLU, 183THR, 184MET, **185ARG**, 186GLU, 187LYS, 188VAL, 189LEU	Fatty acid 1 [31]
3	197LEU, 201SER, 204LYS, 205PHE, 206GLY, 207GLU, **208ARG**, **209ALA**, 210LEU, **211LYS**, **212ALA**, 213TRP, 214SER, **215VAL**, 216ALA, 217ARG, 219SER, **227PHE**, 230VAL, 231THR, 234VAL, 235THR, 238THR, 318TYR, 321ALA, 322LYS, **323ASP**, 324ALA, 325PHE, **326LEU**, 327GLY, 328SER, 329PHE, **330LEU**, 331TYR, 332GLU, 334SER, 342VAL, 343SER, 344VAL, 345LEU, 346LEU, 347ARG, 348LEU, **349ALA**, **350LYS**, 351GLU, 352TYR, **353GLU**, 354ALA, 355THR, 356LEU, 357GLU, 474LYS, 475CYS, 477THR, 478GLU, 479SER, 480LEU, 481VAL, 482ASN, 483ARG, 484ARG, 485PRO, 486CYS	Fatty acid 6 [31]
4	190THR, **191SER**, 192SER, 193ALA, 194ARG, **195GLN**, 196ARG, 197LEU, **198ARG**, 201SER, 205PHE, 209ALA, 210LEU, 212ALA, 213TRP, 214SER, 216ALA, 217ARG, 220GLN, **241HIS**, 340TYR, 341ALA, 342VAL, 343SER, 344VAL, 345LEU, 346LEU, 347ARG, 350LYS, 445MET, 446PRO, 447CYS, 448THR, 449GLU, 450ASP, 451TYR, 452LEU, 453SER, 454LEU, 455ILE, 456LEU, 457ASN, 458ARG, 479SER, 480LEU, 481VAL, 482ASN, 483ARG, 484ARG, 485PRO	Sudlow drug site I [31, 51]
5	383PRO, 386LEU, **387ILE**, 389GLN, **390ASN**, 391CYS, 393GLN, 394PHE, **402PHE**, 403GLN, 405ALA, **406LEU**, 407ILE, **409ARG**, **410TYR**, **413LYS**, 414VAL, 425VAL, 426SER, 427ARG, 428SER, 429LEU, 430GLY, 431LYS, **432VAL**, **433GLY**, 434THR, 435ARG, 436CYS, 448THR, 449GLU, 451TYR, **452LEU**, 453SER, 455ILE, 456LEU, **484ARG**, 485PRO, 486CYS, 487PHE, **488SER**, 489ALA, 490LEU	Sudlow drug site II [31, 51]

6 (Ca)	32GLN, 106LYS, 107ASP, 108ASP, 109SER, 110PRO, 111ASP, 112LEU, 144ARG, 146PRO, 147TYR, 196ARG, 421THR, 458ARG, 459LEU, 460CYS, 461VAL, 462LEU, 463HIS, 464GLU, 465LYS, 466THR	
7 (Ca out)	6GLU, 9HIS, 10ARG, 13ASP, 14LEU, 67HIS, 99ASN, 103LEU, 202ILE, 207GLU, 238THR, 239LYS, 240VAL, 241HIS, 242LYS, 243GLU, 244CYS, 245CYS, 246HIS, 247GLY, 248ASP, 249LEU, 250LEU, 251GLU, 252CYS, 253ALA, 254ASP, 255ASP, 256ARG, 257ALA, 258ASP, 259LEU	

cavity; in bold and green are residues creating the binding pockets according to crystallographic work of Bujacz 2012, while in column 3 is given the name of pocket according to the literature [31,50,51].

Some pockets such as fatty acid 5 were discarded as they are too hydrophobic in the structure of BSA to interact strongly with our charged ligands [32]. The sites that are responsible for binding cations are added in the study considering that most of our ligands are small positively charged molecules.

All conformations of all ligands were docked in all seven selected pockets using Triangle Matcher algorithm for initial placement of structures which returns up to 10E4 poses of a ligand inside a pocket. These poses were scored by London dG [MOE] (Molecular Operating Environment (MOE). Chemical Computing Group, Montreal, Quebec, Canada] function which estimates the free energy of binding of the ligand from a given pose and consists of terms that estimates average gain/loss of rotational and translational entropy and loss of flexibility of the ligand, measures geometric imperfections of hydrogen bonds and desolvation energy of the atom.

The best 50 poses for every ligand for every pocket were further optimized with Induced Fit methodology using MMFF94 force field and optimization cut-off of 6A from the ligand. The GBVI/WSA dG [MOE] was used as a rescoring function and the best 50 poses were collected for further analysis. The interaction energies of ligands in different pockets based on the GBVI/WSA dG scoring function were sorted and 5 best pockets for every ligand according to ligand-pocket interactions were selected.

The cluster analysis was done on a set of interactions between ligands and atoms in every one of the specified pockets. The first 10 clusters ordered by their lowest energy participants were selected and their lowest energy participants were further optimized using MMFF94. Residues that have atoms closer than 9A to the ligand were considered free during an energy minimization, while other residues were tethered.

3. Results and discussion

3.1. Synthesis, identification, and characterization of the [L-AAOR][NAP]

The amino acid ester naproxenate were obtained as white powders in high yields (92.0–98.5%) (Table 2). The structure and purity of the compounds were confirmed by ^{1}H NMR, ^{13}C NMR, FTIR, and elemental analysis. In the ^{1}H NMR spectra is observed a singlet with a chemical shift in the range between 4.52 ppm for [L-ValOBu][NAP] to 6.21 ppm for [L-LeuOEt][NAP], which corresponds to the protonated amino group of amino acid ester (Supplementary, Fig. S1). The integration of these signals corresponds to three protons. In the ^{13}C NMR spectra, the lower chemical shift (about 2 ppm) of the carbonyl carbon signal for naproxen derivatives in comparison to that for the parent acid form is another confirmation of the ionic structure of the obtained compounds. For the naproxen, this signal is localized at 181.00 ppm, while for [L-AAOR][NAP] – at about 179 ppm [23,52–54]. Additionally, the ionic structure of the novel compounds is found from the presence of strong bands at *ca.* 1570 and 1390 cm^{-1} in FTIR spectra, assigned to the symmetric ($\nu_{sym.}$) (COO^{-}) and asymmetric ($\nu_{as.}$) (COO^{-}) stretching vibrations of carboxylate anion, respectively [55–57]. The FTIR spectra of naproxen and its derivatives are presented for comparison in the

Table 2
Yields of the synthesized L-amino acid alkyl ester naproxenates ([L-AAOR][NAP]).

No.	Compound	Substrate	Product		
		L-AAOR [g]	[L-AAOR][NAP] [g]	Yield [%]	State
1	[L-LeuOEt][NAP]	0.52	1.20	93.7	White solid
2	[L-ValOEt][NAP]	0.75	1.81	93.5	White solid
3	[L-ValOiPr][NAP]	0.83	2.00	98.5	White solid
4	[L-ValOPr][NAP]	0.70	1.66	97.0	White solid
5	[L-ValOBu][NAP]	0.64	1.37	92.0	White solid

Table 3
The melting points and thermal stability of naproxen and its amino acid ester derivatives.

Compound	T_m (°C)	T_{onset} (°C)	$[\alpha]_\lambda^T$	$[M]_\lambda^T$
NAP	153.2–155.6	249.9	+50.99	+117.41
[L-LeuOEt][NAP]	129.1–132.4	120.1	+29.05	+113.11
[L-ValOEt][NAP]	131.8–133.6	121.2	+29.63	+111.25
[L-ValOiPr][NAP]	132.4–134.5	112.1	+30.74	+120.87
[L-ValOPr][NAP]	116.2–118.2	77.7	+31.03	+11,973
[L-ValOBu][NAP]	101.1–103.9	109.4	+29.75	+120.05

T_m—melting point; T_{onset}—the onset of the thermal degradation; $[\alpha]_\lambda^T$ specific rotation; $[M]_\lambda^T$ – molar specific rotation.

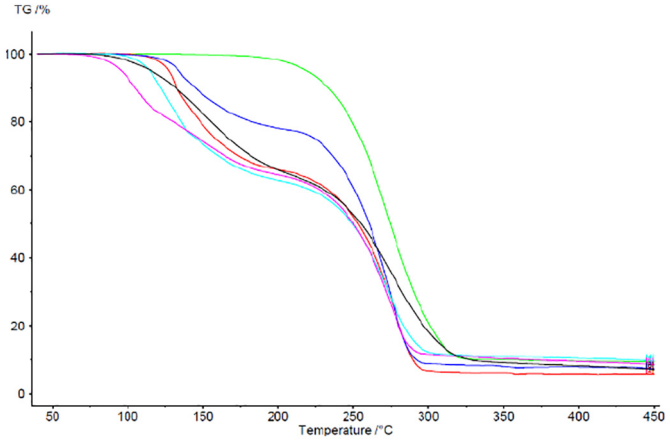

Fig. 1. The thermal gravimetric curves of naproxen and its amino acid ester derivatives, red [L-LeuOEt][NAP]; dark blue [L-ValOEt][NAP]; light blue [L-ValOiPr][NAP]; rose [L-ValOPr][NAP]; black [L-ValOBu][NAP] and green NAP.

Table 4
The solubility of naproxen and its amino acid ester derivatives in water and organic solvents at 25 °C.

Compound	Water (63.1)	Ethanol (51.9)	DMSO (45.1)	Chloroform (39.1)	Ethyl acetate (38.1)	Diethyl ether (34.5)	Toluene (33.9)	n-hexane (31.0)
NAP	−	+	+	+/−	+/−	+/−	−	−
[L-LeuOEt][NAP]	−	+/−	+	+/−	−	−	−	−
[L-ValOEt][NAP]	−	+	+	+/−	+/−	−	−	−
[L-ValOiPr][NAP]	−	+/−	+	+	−	+/−	−	−
[L-ValOPr][NAP]	−	+	+	+	+/−	−	+/−	−
[L-ValOBu][NAP]	−	+	+	+	+	+/−	+/−	−

Solvents were ranked with decreasing value of empirical solvent polarity parameters, ET(30) [58] (Reichardt C, Welton T, Solvents and Solvent Effects in Organic Chemistry, Fourth Edition, Wiley-VCH Verlag GmbH & Co. KGaA, Weinheim 2011) ("+": soluble >100 mg cm^{-3}; "+/−": partially soluble 33–100 mg cm^{-3}; "-": practically insoluble <33 mg cm^{-3}) at the temperature of 25 °C by modified Vogel's method.

Supplementary (Fig. S3). The elemental analysis confirmed the content of individual elements (C, H, N, O) in the synthesized [L-AAOR][NAP].

The [L-AAOR][NAP] are white solids at room temperature and their melting points are given in Table 3. The melting point within the series of L-valine alkyl ester naproxenates decreases with increasing the alkyl chain length in the ester group of amino acid (Table 3). The elongation of the alkyl chain by a CH_2 group each time causes a decrease in the melting point of about 15 °C. However, the secondary alkyl group (*i*-Pr) results in a higher melting point than the primary *n*-propyl one. The same trend was observed earlier for the amino acid ester ketoprofenates [27]. The thermal gravimetric analysis shows two steps of thermal weight loss for naproxen derivatives, while for the parent acid naproxen it is only one. The onset temperature (T_{onset}) for the thermal weight loss of the compounds were determined and presented in Table 3. T_{onset} for the [L-AAOR][NAP] was within the range of 77.7 to 121.2 °C, whereas the value for NAP was 249.9 °C. Thus, the synthesized naproxen-based salts showed lower thermal stability than the parent acid NAP. No direct relationship of thermal stability was found with the increasing length of alkyl chain in ester group of amino acid cation. [L-ValOEt][NAP] and [L-ValOiPr][NAP] had the highest thermal stability, while [L-ValOPr][NAP] was the compound with the lowest thermal stability (Fig. 1). The structure of the amino acid side-chain had an only small effect on the stability of the naproxen derivatives – slightly higher stability was established for the L-valine ethyl ester cation than that for L-leucine ethyl ester. All obtained naproxen-based amino acid ester salts are chiral (two chiral centers) with specific rotation listed in Table 2 [58]. The specific rotation was similar for all obtained compounds and it was found to be between +29.05 for [L-LeuOEt][NAP] and +31.03 for [L-ValOPr][NAP].

The solubility in water and conventional organic solvents are investigated by Vogel's methodology and are summarized in Table 4. The solvents are ranked with decreasing value of empirical polarity parameter ($E_T(30)$). Based on solubility, the compounds are grouped into three categories: the compound is recognized as soluble when more than 100 mg of it is dissolved in 1 cm^3; the compound is partly soluble if 33–100 mg of it is dissolved in 1 cm^3; the compound is insoluble when less than 33 mg of a compound is soluble in 1 cm^3. All naproxen derivatives were practically insoluble in non-polar solvents such as n-hexane. Generally, the obtained compounds were soluble or partly soluble in ethanol, dimethyl sulfoxide, and chloroform. Most of them were insoluble or partly soluble in ethyl acetate, diethyl ether, and toluene.

3.2. Cytotoxicity of the amino acid ester salts of naproxen on murine macrophages

We assessed the effect of [L-AAOR][NAP] on the viability of RAW 264.7 macrophages after 24-h incubation with different concentrations

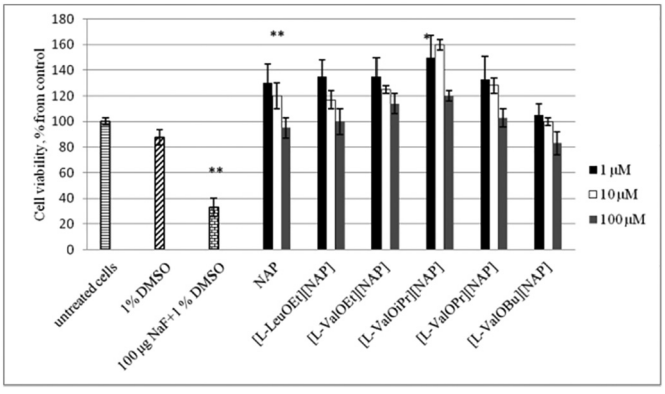

Fig. 2. The effect of amino acid ester naproxenate salts on the percentage of cell viability in RAW 264. 7 macrophages. Control cells were treated with media alone. Values are the mean ± standard error of the mean of three independent experiments. $^{**}P < 0.01$, $^{*}P < 0.05$.

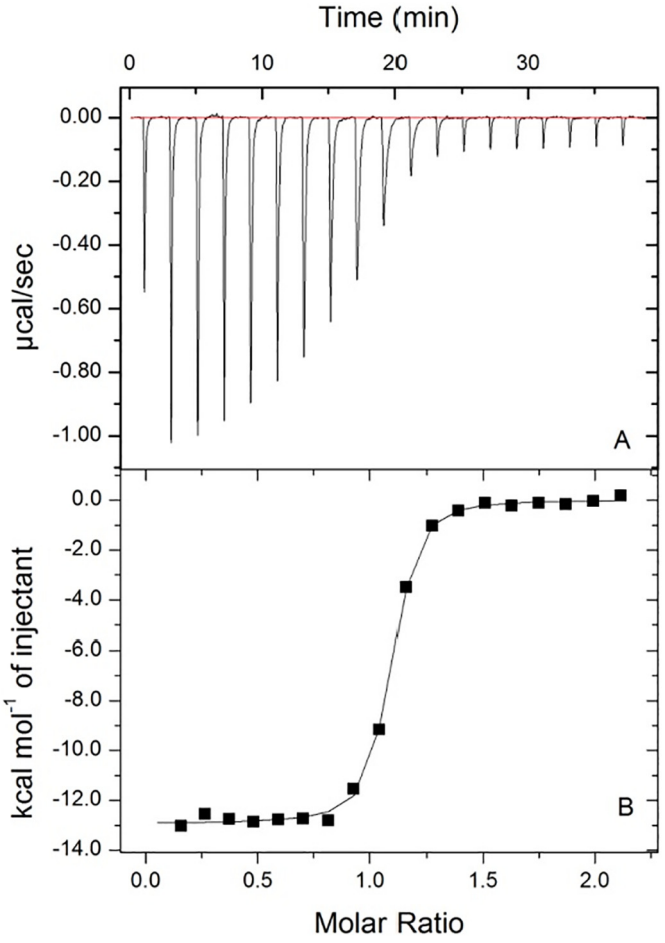

Fig. 3. Calorimetric titration of BSA with NAP (A). Binding isotherm for titration of BSA (32.5 μM) with NAP (0.5 mM) (B). The line is the best-fit curve obtained by using a single type of independent sites model. T = 298.15 K. 20 mM PBS buffer (pH 7.4) with 1% DMSO.

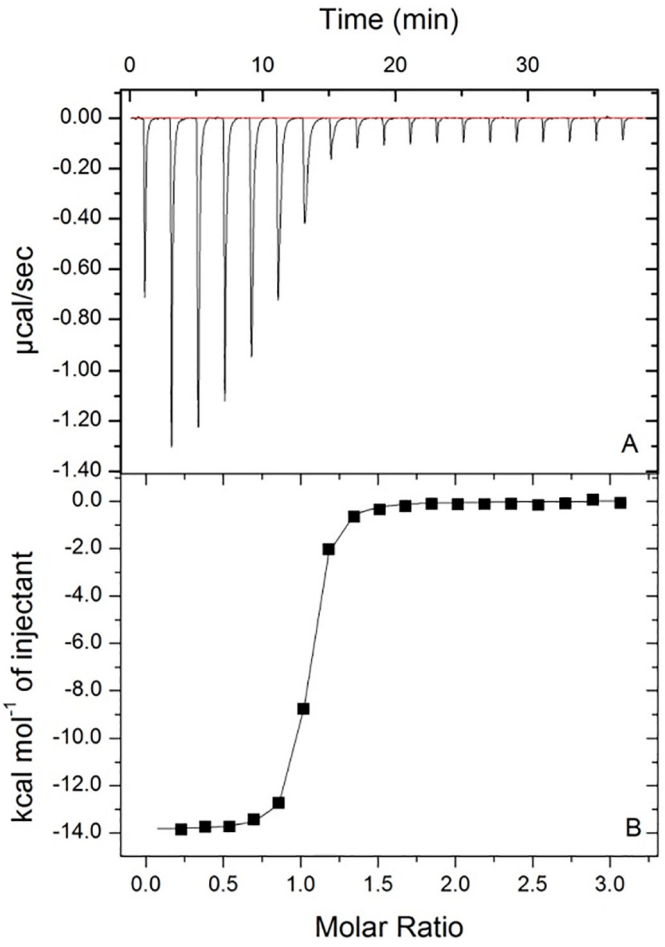

Fig. 4. Calorimetric titration of BSA with [L-ValOEt][NAP] (A). Binding isotherm for titration of BSA (27 μM) of with [L-ValOEt][NAP] (0.6 mM) (B). The line is the best-fit curve obtained by using a single type of independent sites model. T = 298.15 K. 20 mM PBS buffer (pH 7.4) with 1% DMSO.

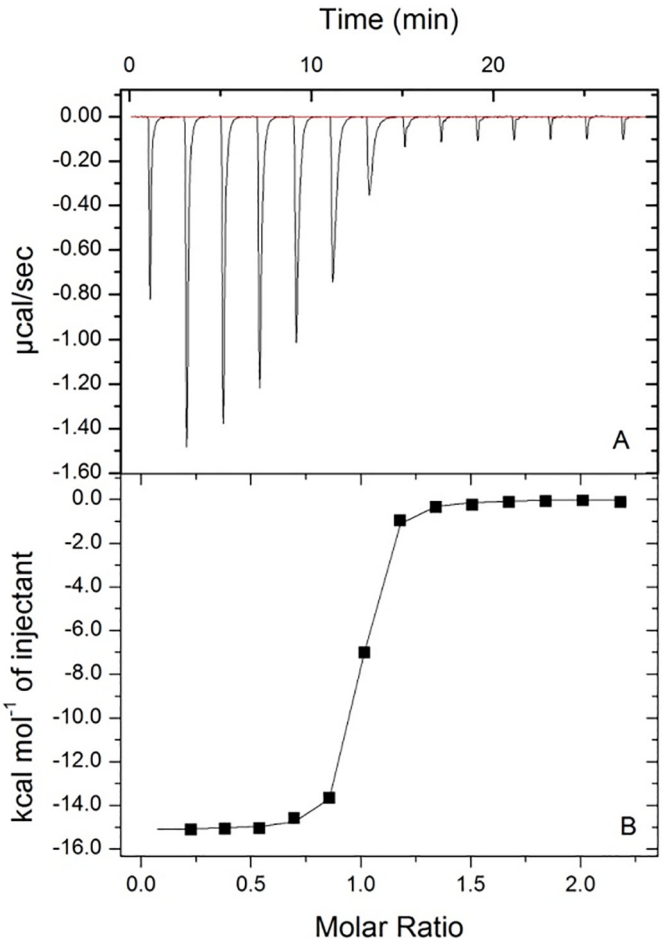

Fig. 5. Calorimetric titration of BSA with [L-ValOPr][NAP] (A). Binding isotherm for titration of BSA (32 μM) of with [L-ValOPr][NAP] (0.5 mM) (B). The line is the best-fit curve obtained by using a single type of independent sites model. T = 298.15 K. 20 mM PBS buffer (pH 7.4) with 1% DMSO.

of the compounds (1, 10, and 100 μM). As controls were used untreated cells, cells treated with 1% DMSO (the solvent in which the compounds are prepared) and 100 μg NaF and 1% DMSO. As seen in Fig. 2 at the tested concentrations, the compounds were safe for macrophages. Moreover, the compounds even were able to stimulate cell proliferation and to minimize the toxic effect of the solvent.

3.3. Thermodynamics of the binding interactions of NAP and its derivatives to BSA

The interactions of BSA with NAP and its amino acid ester salts are investigated by means of ITC. The obtained calorimetric titration curves (A) and the corresponding binding isotherms (B) are given in Figs. 3–8. Each peak in the binding isotherms (panel A) represents a single injection of the ligand into the BSA solution. The parameters and energetics of the binging of NAP and [L-AAOR][NAP] to BSA are summarized in Table 5.

The negative heat deflections, which are observed in the raw data of the isothermal titrations (Figs. 3A–8A), are indications that the binding of NAP and its derivatives with BSA is an exothermic process. The formation of the complexes of BSA with NAP and its amino acid ester salts is a spontaneous process ($\Delta G < O$) and probably conformational change in BSA occurs upon binding of the ligands. Except for [L-ValOiPr][NAP], the binding of NAP and the other tested amino acid esters of NAP is primarily driven by enthalpic contributions, whereas $T\Delta S$ contributes unfavorably. These protein-ligand complexes most probably are stabilized by van der Waals interactions and hydrogen bonds. On the other hand, the binding of [L-ValOiPr][NAP] to BSA is both enthalpy and entropy favoured. Besides, the latter complex is formed predominantly due to electrostatic interactions. The estimated dissociation constant for NAP is in the nanomolar range and the result is comparable with those reported in the literature for BSA-NAP complex under similar conditions [59,60]. As a whole, the conversion of acid NAP to amino acid ester salts did not result in a significant change in the binding affinity (Table 4). The stoichiometry of the binding process indicates the presence of a single binding site for NAP, [L-ValOEt][NAP], and [L-LeuOEt][NAP] within BSA at our experimental conditions. A decrease in the binding stoichiometry was observed for L-ValOPr and L-ValOBu derivatives, which possibly can be explained with the binding of NAP moiety in a pocket near the protein surface, which is then interacting *via* its ester group with one BSA molecule and *via* the aromatic ring with an another BSA molecule. Interestingly, two molecules of [L-ValOiPr][NAP] bind on a single set of identical binding sites of one BSA molecule. On one hand, this can be ascribed to a slight expansion of the BSA binding site *i.e.* ligand-induced conformational change in the protein, which offers a larger hydrophobic area for binding and allows accommodation of two drug molecules. For all compounds, the binding constant is in a range of 3.5×10^6 to 1.5×10^7 M^{-1}, which suggests relatively strong binding in BSA (Table 5). It is noteworthy to be mentioned that K_a of L-ValOPr derivative is 5 fold higher than that of

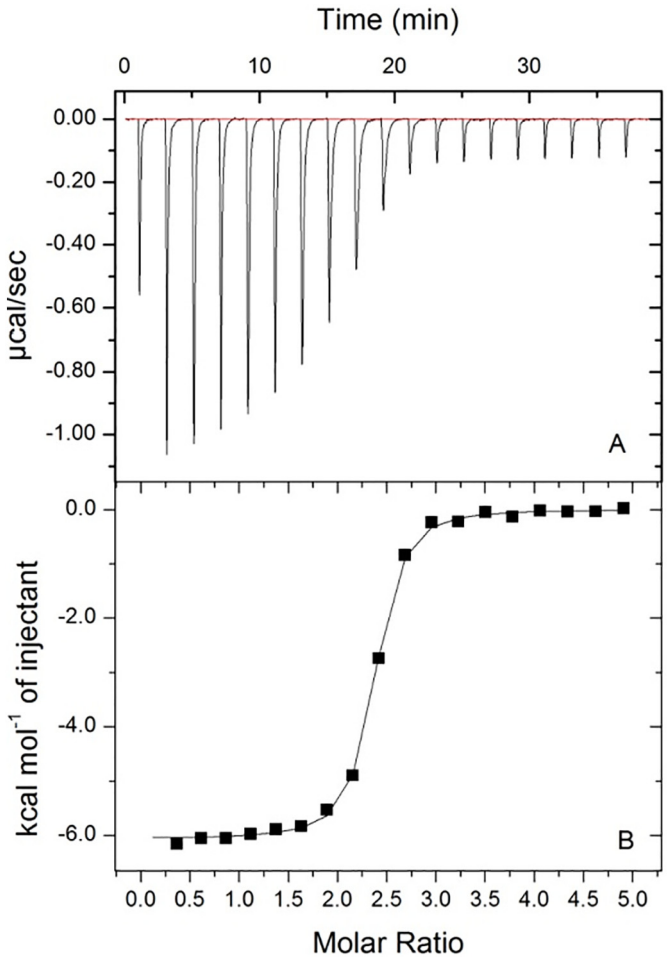

Fig. 6. Calorimetric titration of BSA with [L-ValOiPr][NAP] (A). Binding isotherm for titration of BSA (32.5 μM) of with [L-ValOiPr][NAP] (0.45 mM) (B). The line is the best-fit curve obtained by using a single type of independent sites model. T = 298.15 K. 20 mM PBS buffer (pH 7.4) with 1% DMSO.

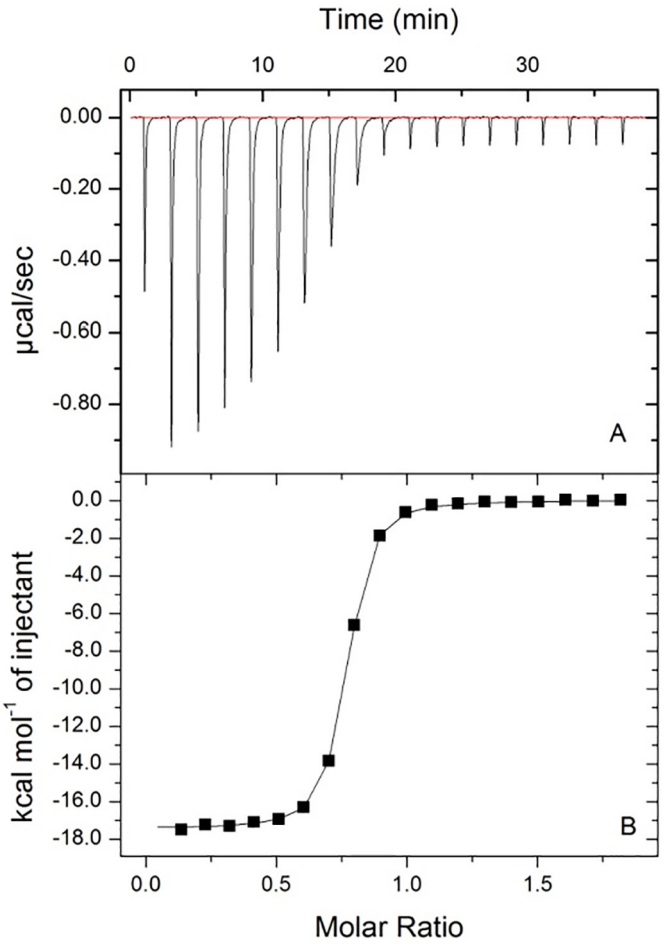

Fig. 7. Calorimetric titration of BSA with [L-ValOBu][NAP] (A). Binding isotherm for titration of BSA (32 μM) of with [L-ValOBu][NAP] (0.5 mM) (B). The line is the best-fit curve obtained by using a single type of independent sites model. T = 298.15 K. 20 mM PBS buffer (pH 7.4) with 1% DMSO.

the isopropyl derivative. From a pharmacokinetic point of view, the lower binding affinity of the [L-ValOiPr][NAP] for albumin suggests a faster diffusion rate in the circulatory system than the parent NAP and other derivatives, and therefore faster reach to the target system.

3.4. Molecular docking studies

The selected most probable seven binding sites of BSA for NAP and its amino acid ester salts are illustrated in Fig. 9.

Typically, the binding of a ligand to one of the pockets can influence binding energies of other ligands to other pockets due to ligand-induced conformational changes in the BSA [61].

3.4.1. Binding of the naproxen moiety

The comparison of energies from the used scoring function – potential energies of interaction between ligands and binding pockets, according to MMFF94 force field, reveals that binding sites used of Ca cations (6 and 7 of our study) are not good enough in the binding of neither naproxen nor of the positively charged ligands.

The negatively charged naproxen best binds in 4, 5, 2, and 1 pockets than other ligands. Its interaction energy in site 4, that is reported as first drug binding site [31], is 5% better than in the other above-mentioned sites, according to MMFF94 potential energy interactions, whereby there is no significant difference between (*S*)- and (*R*)-form of naproxen (Fig. 10). The situation is the same with site 5, which is reported as the second binding site for drugs, [31], where according to our results naproxen binds with slightly lower affinity than in site 4 and (*R*)-naproxen is preferred toward (*S*)-isomer (Fig. 11).

The next preferred binding site for (*S*)-naproxen is site 2, where its binding energy lays between the values of sites 4 and 5. In this binding site the (*S*)-form of naproxen is preferred, while the (*R*)-form has lower energy of interaction and different favoured positions due to steric hindrance with amino acids forming the binding pocket and its interaction energy is lower than interaction energy of (*R*)-naproxen with site 5. Our model shows that in site 2 the carboxyl group of (*R*)-NAP is involved in electrostatic interactions with Arg144 Lys116 and in π-cation interactions between the naphthyl moiety and Lys116. While in the case of (*S*)-NAP, Arg185 and Lys116 stabilize the complex *via* electrostatic and polar-π interactions with carboxylic group and naphthalene ring, respectively. Our results are consistent with the known characteristics of pocket 2. It possesses a positively charged entrance thus providing a good binding environment for negatively charged ligands as naproxen. Moreover, it also has the ability to accommodate its shape to smaller ligands [31].

Naproxen also complex to binding site 1 but with lower affinity than sites 4, 5, and 2 and there is no significant difference between binding of (*R*)- and (*S*)-isomers of naproxen.

The naproxen isomers do not have a high affinity to binding pocket number 3, which is the preferred one for our positively charged ligands, due to the proximity of negatively charged amino acids.

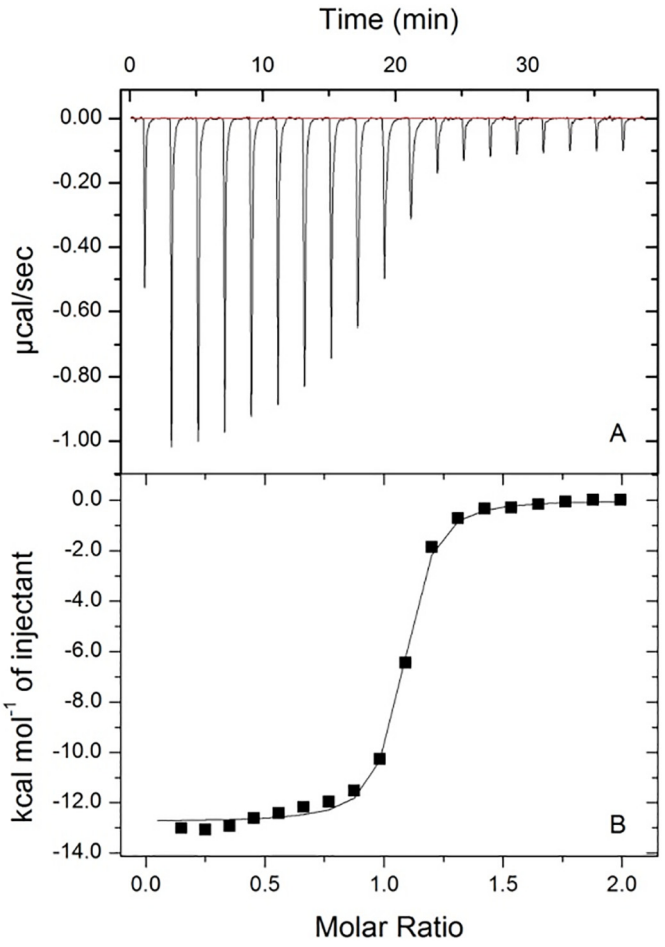

Fig. 8. Calorimetric titration of BSA with [L-LeuOEt][NAP] (A). Binding isotherm for titration of BSA (32 µM) of with [L-LeuOEt][NAP] (0.23 mM) (B). The line is the best-fit curve obtained by using a single type of independent sites model. T = 298.15 K. 20 mM PBS buffer (pH 7.4) with 1% DMSO.

In general, the negatively charged NAP prefers binding in positions in which its negatively charged carboxyl group interacts with positively charged residues inside the binding pockets of albumin.

3.4.2. Binding of the amino acid esters

The positively charged ligands, due to their structural similarity have similar preferences about binding pockets of BSA. For all amino acid esters, the preferred binding site of BSA is site 3.

The best interactions in that binding pocket are the same for all of our cationic ligands. The positively charged amino group participates in hydrogen bonds and ionic interactions with Asp323 and Glu353, and the carboxyl oxygen atom participates in hydrogen bonding with Arg208, while the other part of the binding pocket is mainly lipophilic.

Table 5
Thermodynamic binding parameters for the interaction of NAP and its aminoacid ester salts with BSA in 20 mM phosphate buffer saline (pH 7.4) containing 1% DMSO at 298.15 K.

Compound	N	Ka µM	K_d nM	ΔH kcal/mol	ΔS cal/mol K	ΔG kcal/mol
NAP	1.0	11.2	90.7	−13.16	−11.9	−9.61
[L-LeuOEt][NAP]	1.1	12.2	81.7	−12.54	−9.63	−9.68
[L-ValOEt][NAP]	1.1	12.3	81.3	−13.63	−13.2	−9.69
[L-ValOiPr][NAP]	2.2	3.5	281.0	−5.98	9.9	−8.83
[L-ValOPr][NAP]	0.8	15.6	64.0	−16.45	−22.2	−9.84
[L-ValOBu][NAP]	0.8	12.3	80.7	−16.6	−23.3	−9.38

The peculiar geometry of the pocket enables positioning of lipophilic alkyl groups of ligands in a way that they contact with similarly lipophilic parts at both ends of the BSA pocket, while at the same time the outer part of the ligand is exposed to the water solvent. The difference in binding energy among ligands and this binding site of the albumin molecule is due mainly to the different sizes of aliphatic parts and their lipophilic interactions with lipophilic residues of the albumin molecule. As the site is open in both sides to the solvent, the aliphatic parts of ligands have no steric hindrances with some residues from the pocket.

The interaction energies between positively charged ligands and binding site 4 are 25 to 70% less energetically favorable but their best positions in binding site 5 have two to four orders of magnitude lower binding energies due to the lack of negatively charged groups inside the pocket and many positively charged ones.

Because site 3 is in close proximity of site 4 and they share BSA residues, it is possible that binding of naproxen in site 4 will deform site 3 in such a way that our cation ligand will not prefer binding to site 3. To check this we perform a new docking study in which we dock cation ligands in binding site 3, while naproxen molecule is bound in binding pocket 4, whose geometry is from the last optimization of induced fit docking procedure, but we do not observe significant changes in binding of the ligands in site 3.

Some other problems with the selection of the exact best place for binding cationic ligands in site 3 are that Asp323, Arg208, and Glu353 belong to different α-helices that move one to another. Additional optimization showed that site 3 participates more with lowering of the temperature, but at 37 °C despite having high interaction energy in optimal positions of the alpha spirals our cations will not be settled on that site for longer than 100 ns because of thermal movement of the molecule so site 3 will probably not be the most important participant in overall BSA capability to form complexes with our positively charged ligands (Fig. 12).

As the binding energy of NAP within site 4 is more than two times better compared to our cationic ligands, more likely this site is occupied by NAP than that the cationic ligands.

The cation ligands can bind in the next preferred site, namely site 1, where NAP molecule also binds better than them but because they are salts with an equal amount of the cation and the anion this site should be free for interaction.

This site also consists of optimally positioned two acidic residues (Glu152 and Glu291), and one basic residue (Arg198) to bind our cationic ligands as shown for L-ValOEt on Fig. 13.

It is noteworthy to be mentioned that site 1 residues involved in the interactions are positioned in a relatively narrow hollow and due to steric hindrance with Arg198, His241 and Tyr 149 this site is unfavorable for branched aliphatic cations.

Site 1 is also far most stable during the molecular dynamics simulation with RMSD of alpha carbon atoms during the 50 ns trajectory 0.68A that suggests for good stability of the formed complexes.

4. Conclusions

Five novel naproxen-based amino acid ester salts not toxic to immune cells were synthesized and thoroughly characterized. Molecular docking experiment showed that four binding sites of bovine serum albumin are appropriate to accommodate both the cation and anion and ensure relative strong binding interaction with the closely located and appropriately oriented amino acid moieties comprising the binding pockets. Only L-valine isopropyl ester naproxenate, due to steric hindrance, characterizes with about one order of magnitude lower binding affinity for albumin, which suggests a faster diffusion rate in the circulatory system than the parent NAP and other derivatives, and therefore faster reach to the target system. This makes the compound promising for the development of a formulation with a faster onset of action.

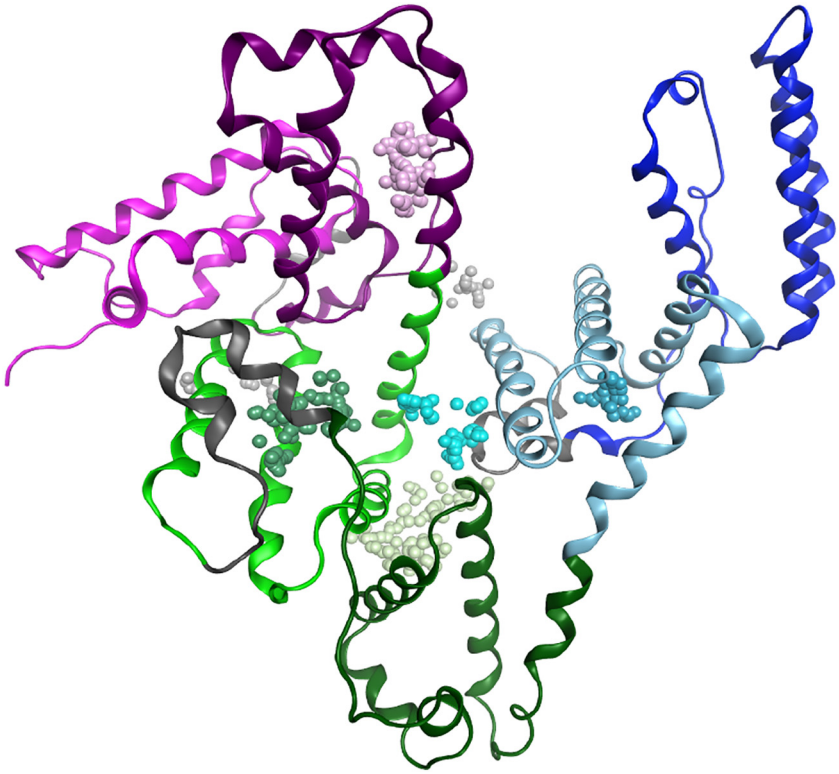

Fig. 9. One of the structures from MD used in our docking study painted according to [50]. Defined in our study binding pockets are represented with colored balls placed in placement points used in the docking process Site 1 is depicted with green, Site 2 in pink, Site 3 in light green, Site 4 in cyan, Site 5 in blue Site 6 and 7 are in gray.

CRediT authorship contribution statement

P·O, E.Y., J.K., E.S contributed to the synthesis and physic-chemical characterization of the compounds. P.K., S.T, E.K. carried out protein-ligand interaction studies. M.R. and N.T. performed molecular docking studies. M.G. performed cytotoxicity studies. P.O., E.Y, M.R and M.G did interpretation of the results. M.G. took the lead in writing the manuscript. All authors provided critical feedback and helped shape the research, analysis and manuscript.

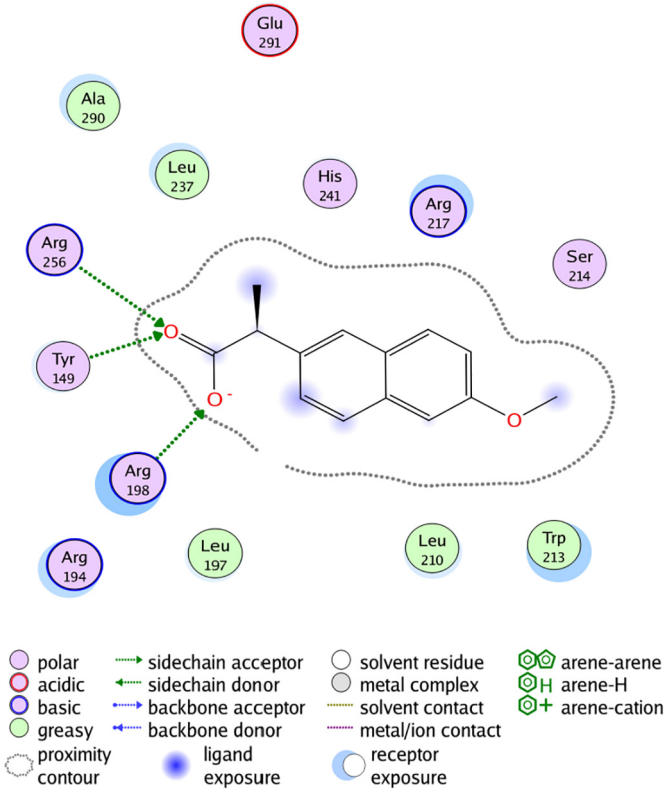

Fig. 10. The interaction map of (*S*)-Naproxen in its preferred position in binding site 4.

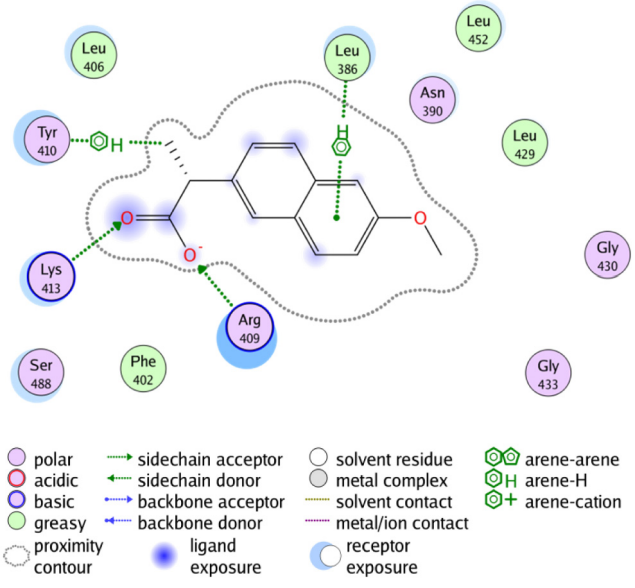

Fig. 11. The interaction map of (*R*)-Naproxen in its preferred position in binding site 5.

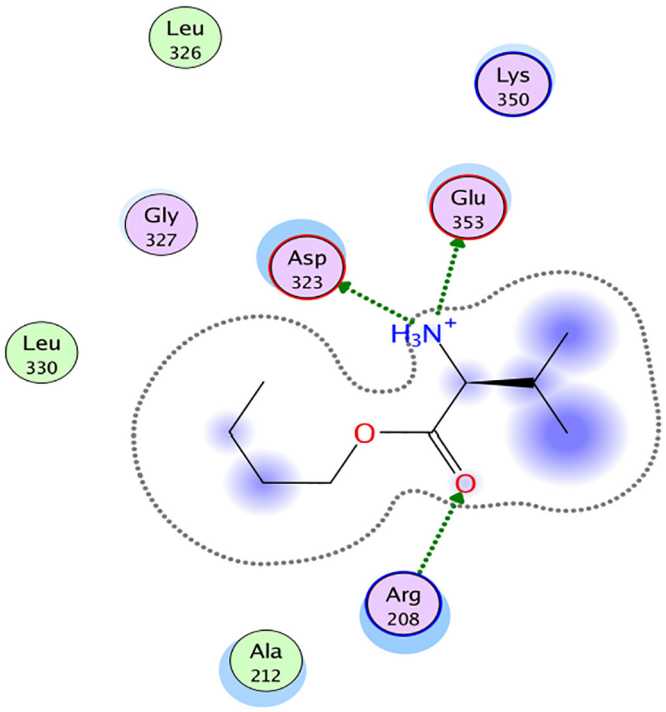

Fig. 12. The interaction map of one of the ligands in the best interaction position in the site 3.

Declaration of competing interest

The authors declare no conflict of interest.

Acknowledgments

This work was partially supported by the Bulgarian Ministry of Education and Science under the National Research Programme "Young scientists and postdoctoral students" approved by DCM # 577/17.08.2018.

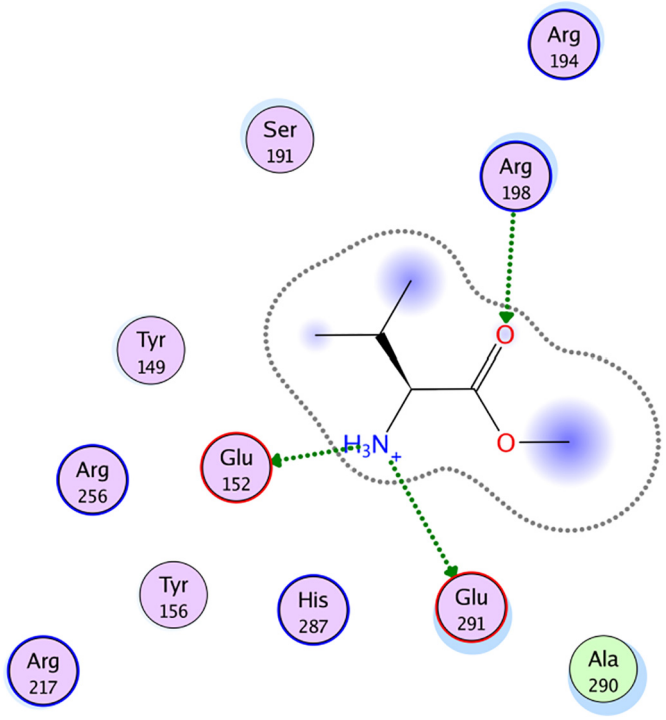

Fig. 13. The interaction map of L-ValOEt in site 1.

Appendix A. Supplementary data

Supplementary data to this article can be found online at https://doi.org/10.1016/j.molliq.2020.114283.

References

[1] T. Welton, Ionic liquids: a brief history, Biophys. Rev. 10 (2018) 691–706, https://doi.org/10.1007/s12551-018-0419-2.
[2] M. Draye, G. Chatel, R. Duwald, Ultrasound for drug synthesis: a green approach, Pharmaceuticals 13 (2020) 23, https://doi.org/10.3390/ph13020023.
[3] C. Guo, J. Zhang, C. Liu, Y. Bian, Q. Shan, Extracting rose essential oil from rose slag with ionic liquid, Biomass Convers. Biorefin. (2020)https://doi.org/10.1007/s13399-020-00751-9.
[4] P. Berton, M.K. Mishra, H. Choudhary, A.S. Myerson, R.D. Rogers, Solubility studies of cyclosporine using ionic liquids, ACS Omega 4 (2019) 7938–7943, https://doi.org/10.1021/acsomega.9b00603.
[5] H. Almeida, M. Freire, I. Marrucho, Improved monitoring of aqueous samples by the preconcentration of active pharmaceutical ingredients using ionic-liquid-based systems, Green Chem. 19 (2017) 4651–4659, https://doi.org/10.1039/C7GC01954H.
[6] K. Egorova, E. Gordeev, V. Ananikov, Biological activity of ionic liquids and their application in pharmaceutics and medicine, Chem. Rev. 117 (2017) 7132–7189, https://doi.org/10.1021/acs.chemrev.6b00562.
[7] Z. Sidat, T. Marimuthu, P. Kumar, L.C. du Toit, P.P.D. Kondiah, Y.E. Choonara, V. Pillay, Ionic liquids as potential and synergistic permeation enhancers for transdermal drug delivery, Pharmaceutics 11 (2019) 96, https://doi.org/10.3390/pharmaceutics11020096.
[8] V. Fernandez-Stefanuto, E. Tojo, New active pharmaceutical ingredient-ionic liquids (API-ILs) derived from indomethacin and mebendazole, Proceedings 9 (2019) 48, https://doi.org/10.3390/ecsoc-22-05781.
[9] R.Md. Moshikur, Md.R. Chowdhury, R. Wakabayashi, Y. Tahara, M. Moniruzzaman, M. Goto, Ionic liquids with methotrexate moieties as a potential anticancer prodrug: synthesis, characterization and solubility evaluation, J. Mol. Liq. 278 (2019) 226–233, https://doi.org/10.1016/j.molliq.2019.01.063.
[10] H. Wu, Z. Deng, B. Zhou, M. Qi, M. Hong, G. Ren, Improved transdermal permeability of ibuprofen by ionic liquid technology: correlation between counterion structure and the physicochemical and biological properties, J. Mol. Liq. 283 (2019) 399–409, https://doi.org/10.1016/j.molliq.2019.03.046.
[11] H. Wu, F. Fang, L. Zheng, W. Ji, M. Qi, M. Hong, G. Ren, Ionic liquid form of donepezil: preparation, characterization and formulation development, J. Mol. Liq. 300 (2019) 112308, https://doi.org/10.1016/j.molliq.2019.112308.
[12] Y. Sahbaz, H. Williams, T.-H. Nguyen, J. Saunders, L. Ford, S. Charman, P. Scammells, C. Porter, Transformation of poorly water-soluble drugs into lipophilic ionic liquids enhances oral drug exposure from lipid based formulations, Mol. Pharm. 12 (2015) 1980–1991, https://doi.org/10.1021/mp500790t.
[13] H. Park, M. Prausnitz, Lidocaine-ibuprofen ionic liquid for dermal anesthesia, AIChE J. 61 (9) (2015) 2732–2738, https://doi.org/10.1002/aic.14941.
[14] D. Monti, E. Egiziano, S. Burgalassi, P. Chetoni, C. Chiappe, A. Sanzone, S. Tampucci, Ionic liquids as potential enhancers for transdermal drug delivery, Int. J. Pharm. 516 (2017) 45–51, https://doi.org/10.1016/j.ijpharm.2016.11.020.
[15] J. Shamshina, P. Barber, R.D. Rogers, Ionic liquids in drug delivery, Expert Opin. Drug Deliv. 10 (10) (2013) 1367–1381, https://doi.org/10.1517/17425247.2013.808185.
[16] Q. Zheng, A. Mukherjee, P. Müller, R.D. Rogers, A. Myerson, Exploring the role of ionic liquids to tune the polymorphic outcome of organic compounds, Chem. Sci. 9 (2018) 1510–1520, https://doi.org/10.1039/C7SC04353H.
[17] X. Zhao, Q. Li, C. Wang, S. Hu, X. He, C.C. Sun, Simultaneous taste-masking and oral bioavailability enhancement of Ligustrazine by forming sweet salts, Int. J. Pharm. 577 (2020), 119089, https://doi.org/10.1016/j.ijpharm.2020.119089.
[18] S. Wongrakpanich, A. Wongrakpanich, K. Melhado, J.A. Rangaswami, Comprehensive review of non-steroidal anti-inflammatory drug use in the elderly, Aging Dis. 9 (1) (2018) 143–150, https://doi.org/10.14336/AD.2017.0306.
[19] M. Munir, C. Eli, Z. J.-Ming, in: Howard E. Smith (Ed.), Chapter 60 Nonsteroidal Anti-Inflammatory Drugs and Cyclooxygenase-2 Inhibitors in Current Therapy in Pain, E-book, Saunders, Elsevier, 2009.
[20] A. Azevedo, S. Costa, A. Dias, A. Marques, P. Pinto, K. Bica, A. Ressmann, M. Passos, A. Araújo, S. Reis, M.L. Saraiva, Anti-inflammatory choline based ionic liquids: insights into their lipophilicity, solubility and toxicity parameters, J. Mol. Liq. 232 (2017) 20–26, https://doi.org/10.1016/j.molliq.2017.02.027.
[21] M. Santos, L. Raposo, G. Carrera, A. Costa, M. Dionísio, P. Baptista, A. Fernandes, L. Branco, Ionic liquids and salts from ibuprofen as promising innovative formulations of an old drug, ChemMedChem 14 (9) (2019) 907–911, https://doi.org/10.1002/cmdc.201900040.
[22] R.Md. Moshikur, Md.R. Chowdhury, R. Wakabayashi, Y. Tahara, N. Kamiya, M. Moniruzzaman, M. Goto, Ionic liquids with N-methyl-2-pyrrolidonium cation as an enhancer for topical drug delivery: synthesis, characterization, and skin penetration evaluation, J. Mol. Liq. 299 (2020), 112166, https://doi.org/10.1016/j.molliq.2019.112166.
[23] E. Janus, P. Ossowicz, J. Klebeko, A. Nowak, W. Duchnik, Ł. Kucharski, A. Klimowicz, Enhancement of ibuprofen solubility and skin permeation by conjugation with L-valine alkyl esters, RSC Adv. 10 (2020) 7570–7584, https://doi.org/10.1039/D0RA00100G.
[24] Y. Zhang, Y. Cao, X. Meng, Ch. Li, H. Wang, S. Zhang, Enhancement of transdermal delivery of artemisinin using microemulsion vehicle based on ionic liquid and

lidocaine ibuprofen, Colloids Surf. B: Biointerfaces 189 (2020), 110886, https://doi.org/10.1016/j.colsurfb.2020.110886.
[25] F. Parra-Ruiz, E. Toledano, M. Fernández-Gutiérrez, N. Dinjaski, M.A. Prieto, B. Vázquez-Lasa, J.S. Román, Polymeric systems containing dual biologically active ions, Eur. J. Med. Chem. 46 (2011) 4980–4991, https://doi.org/10.1016/j.ejmech.2011.08.004.
[26] R. Ribeiro, P. Pinto, A. Azevedo, K. Bica, A. Ressmann, S. Reis, M.L. Saraiva, Automated evaluation of protein binding affinity of anti-inflammatory choline based ionic liquids, Talanta 150 (2016) 20–26, https://doi.org/10.1016/j.talanta.2015.12.009.
[27] P. Ossowicz, P. Kardaleva, M. Guncheva, J. Klebeko, E. Swiatek, E. Janus, D. Yancheva, I. Angelov, Ketoprofen-based ionic liquids: synthesis and interactions with bovine serum albumin, Molecules 25 (2020) 90, https://doi.org/10.3390/molecules25010090.
[28] P.P. Misra, N. Kishore, Differential modulation in binding of ketoprofen to bovine serum albumin in the presence and absence of surfactants: spectroscopic and calorimetric insights, Chem. Biol. Drug Des. 82 (2013) 81–98, https://doi.org/10.1111/cbdd.12136.
[29] D. Khaibrakhmanova, A. Nikiforova, I. Sedov, Binding constants of substituted benzoic acids with bovine serum albumin, Pharmaceuticals 13 (2020) 30, https://doi.org/10.3390/ph13020030.
[30] B. Vaidya, N.S. Kulkarni, S. Shukla, V. Parvathaneni, G. Chauha, J. Damon, A. Sarode, J. Garcia, N. Kunda, S. Mitragotri, V. Gupta, Development of inhalable quinacrine loaded bovine serum albumin modified cationic nanoparticles: repurposing quinacrine for lung cancer therapeutics, Int. J. Phar. 577 (2020) 118995, https://doi.org/10.1016/j.ijpharm.2019.118995.
[31] A. Bujacz, K. Zielinski, B. Sekula, Structural studies of bovine, equine, and leporine serum albumin complexes with naproxen, Proteins 82 (9) (2014) 2199–2208, https://doi.org/10.1002/prot.24583.
[32] A.J. Ryan, J. Ghuman, P.A. Zunszain, C.W. Chung, S. Curry, Structural basis of binding of fluorescent, site-specific dansylated amino acids to human serum albumin, J. Struct. Biol. 174 (1) (2011) 84–91, https://doi.org/10.1016/j.jsb.2010.10.004.
[33] N. Vale, A. Ferreira, J. Matos, P. Fresco, M.J. Gouveia, Amino acids in the development of prodrugs, Molecules 23 (2018) 2318, https://doi.org/10.3390/molecules23092318.
[34] B.H. Furniss, A.J. Hannaford, P.W.G. Smith, A.R. Tatchell, Vogel's Textbook of Practical Organic Chemistry, fifth ed. Longman Scientific & Technical, John Wiley &Sons, Inc, New York, 1989.
[35] H.M. Berman, J. Westbrook, Z. Feng, G. Gilliland, T.N. Bhat, H. Weissig, I.N. Shindyalov, P.E. Bourne, The Protein Data Bank, Nucleic Acids Res. 28 (2000) 235–242, https://doi.org/10.1093/nar/28.1.235.
[36] P. Emsley, B. Lohkamp, W.G. Scott, K. Cowtan, Features and development of coot, Acta Crystallograph. D, Biol. Crystallograp D66 (2010) 486–501, https://doi.org/10.1107/S0907444910007493 ISSN 0907-4449F.
[37] M.J. Abraham, T. Murtola, R. Schulz, S. Páll, J.C. Smith, B. Hess, E. Lindahl, GROMACS: high performance molecular simulations through multi-level parallelism from laptops to supercomputers, Software X 1-2 (2015) 19–25, https://doi.org/10.1016/j.softx.2015.06.001.
[38] H.J.C. Berendsen, J.P.M. Postma, A. DiNola, J.R. Haak, Molecular dynamics with coupling to an external bath, J. Chem. Phys. 81 (1984) 3684–3690, https://doi.org/10.1063/1.448118.
[39] H.J.C. Berendsen, D. van der Spoel, R. van Drunen, GROMACS: a message-passing parallel molecular dynamics implementation, Comp. Phys. Comm. 91 (1–2) (1995) 43–56, https://doi.org/10.1016/0010-4655(95)00042-E.
[40] G. Bussi, D. Donadio, M. Parrinello, Canonical sampling through velocity rescaling, J. Chem. Phys. 126 (2007), 014101, https://doi.org/10.1063/1.2408420.
[41] B. Hess, C. Kutzner, D. van der Spoel, E. Lindahl, GROMACS 4: algorithms for highly efficient, load-balanced, and scalable molecular simulation, J. Chem. Theory Comput. 4 (2008) 435–447, https://doi.org/10.1021/ct700301q.
[42] E. Lindahl, B. Hess, D. van der Spoel, GROMACS 3.0: a package for molecular simulation and trajectory analysis, J. Mol. Mod 7 (2001) 306–317, https://doi.org/10.1007/s008940100045.
[43] S. Páll, M.J. Abraham, C. Kutzner, B. Hess, E. Lindahl, Tackling exascale software challenges in molecular dynamics simulations with GROMACS, in: S. Markidis, E. Laure (Eds.),Solving Software Challenges for Exascale, vol. 8759, 2015, pp. 3–27.
[44] M. Parrinello, A. Rahman, Polymorphic transitions in single crystals: a new molecular dynamics method, J. Appl. Phys. 52 (1981) 7182–7190, https://doi.org/10.1063/1.328693.
[45] S. Pronk, S. Páll, R. Schulz, P. Larsson, P. Bjelkmar, R. Apostolov, M.R. Shirts, J.C. Smith, P. Kasson, D. van der Spoel, B. Hess, E. Lindahl, GROMACS 4.5: a high-throughput and highly parallel open source molecular simulation toolkit, Bioinformatics 29 (2013) 845–854, https://doi.org/10.1093/bioinformatics/btt055.
[46] D. van der Spoel, E. Lindahl, B. Hess, G. Groenhof, A.E. Mark, H. Berendsen, GROMACS: fast, flexible and free, J. Comp. Chem. 26 (2005) 1701–1719, https://doi.org/10.1002/jcc.20291.
[47] U. Essmann, L. Perera, M.L. Berkowitz, T. Darden, H. Lee, L.G. Pedersen, A smooth particle mesh Ewald method, J. Chem. Phys. 103 (1995) 8577–8592, https://doi.org/10.1063/1.470117.
[48] B. Hess, H. Bekker, H. Berendsen, J. Fraaije, LINCS: a linear constraint solver for molecular simulations, J. Comp. Chem. 18 (1997) 1463–1472, https://doi.org/10.1002/(SICI)1096-987X(199709)18:12<1463::AID-JCC4>3.0.CO;2-H.
[49] S. Miyamoto, P.A. Kollman, SETTLE: an analytical version of the SHAKE and RATTLE algorithms for rigid water models, J. Comp. Chem. 13 (1992) 952–962, https://doi.org/10.1002/jcc.540130805.
[50] Bujacz A. Structures of bovine, equine and leporine serum albumin. Acta Crystallogr. D Biol. Crystallogr. (2012) 68 (Pt 10), 1278–1289. doi:https://doi.org/10.1107/S0907444912027047.
[51] G. Sudlow, D.J. Birkett, D.N. Wade, The characterization of two specific drug binding sites on human serum albumin, Mol. Pharmacol. 11 (1975) 824–832http://molpharm.aspetjournals.org/content/11/6/824.
[52] P. Ossowicz, E. Janus, G. Schroeder, Z. Rozwadowski, Spectroscopic studies of amino acid ionic liquid-supported Schiff bases, Molecules 18 (2013) 4986–5004, https://doi.org/10.3390/molecules18054986.
[53] Z. Rozwadowski, Deuterium isotope effects on 13C chemical shifts of lithium salts of Schiff bases amino acids, J. Mol. Struct. 753 (2006) 127–131, https://doi.org/10.1016/j.molstruc.2005.06.005.
[54] E. Breitmaier, W. Voelter, in: H.F. Ebel (Ed.), Voelter, Monographs in Modern Chemistry, 13C NMR Spectroscopy, Verlag Chemie, Weinheim, 1974.
[55] S. Vairam, T. Premkumar, S. Govindarajan, Trimellitate complexes of divalent transition metals with hydrazinium cation, J. Therm. Anal. Calorim. 100 (2010) 955–960, https://doi.org/10.1007/s10973-009-0459-8.
[56] B. Koleva, T. Kolev, M. Spiteller, Spectroscopic analysis and structural elucidation of small peptides – Experimental and theoretical tools; book chapter, in: J.C. Taylor (Ed.), Advances in Chemistry Research, Book Series, vol. 3, Nova Science Publishers Inc, N.Y., US, 2010.
[57] N. Roeges, A Guide to the Complete Interpretation of Infrared Spectra of Organic Structures, Wiley, 1994.
[58] C. Reichardt, T. Welton, Solvents and Solvent Effects in Organic Chemistry, Fourth edition Wiley-VCH Verlag GmbH & Co. KGaA, Weinheim, 2011.
[59] C. Ràfols, S. Zarza, E. Bosch, Molecular interactions between some non-steroidal anti-inflammatory drugs (NSAID's) and bovine (BSA) or human (HSA) serum albumin estimated by means of isothermal titration calorimetry (ITC)and frontal analysis capillary electrophoresis (FA/CE), Talanta 130 (2014) 241–250, https://doi.org/10.1016/j.talanta.2014.06.060.
[60] T. Banerjee, S.K. Singh, N. Kishore, Binding of naproxen and amitriptyline to bovine serum albumin: biophysical aspects, J. Phys. Chem. B 110 (2006) 24147–24156, https://doi.org/10.1021/jp062734p.
[61] I. Petitpas, T. Grüne, A.A. Bhattacharya, S. Curry, Crystal structures of human serum albumin complexed with monounsaturated and polyunsaturated fatty acids, J. Mol. Biol. 314 (5) (2001) 955–960, https://doi.org/10.1006/jmbi.2000.5208.

1869

БЪЛГАРСКА АКАДЕМИЯ НА НАУКИТЕ

Институт по оптически материали и технологии
“Акад. Йордан Малиновски”

ИОМТ

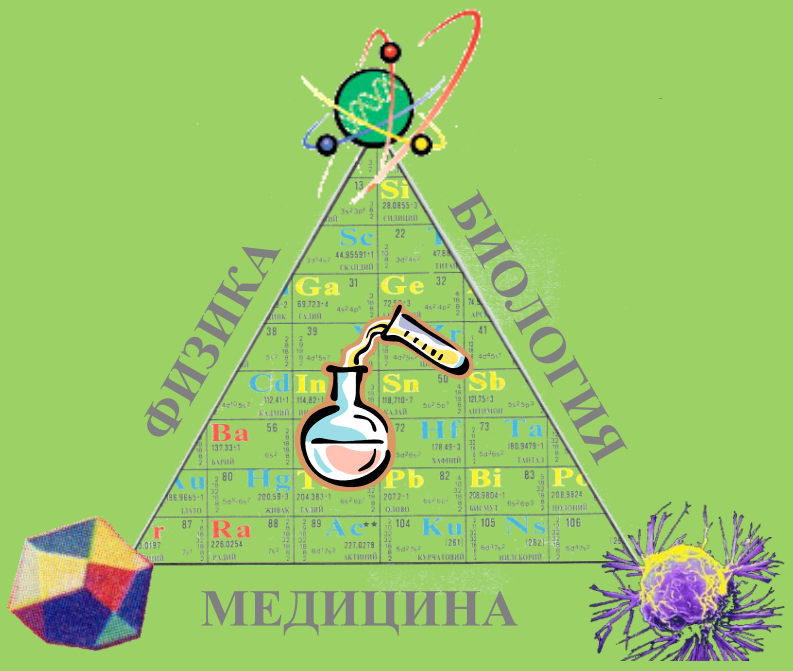

XIII-ти Пролетен семинар - уебинар на младите учени и докторанти от БАН

“ИНТЕРДИСЦИПЛИНАРНА ХИМИЯ”

22-24 юни 2020 г., виртуална зала Moodle/Big Blue Button

XIII-ти Пролетен семинар - уебинар на докторантите и младите учени

“Интердисциплинарна химия”

ПРОГРАМА

22.06.2020		
9:30 – 10:00	доц. д-р Даниела Карашанова - ИОМТ	Откриване
10:00 – 10:45	проф. д-р Маргарита Апостолова - ИМБ	COVID-19: OPENING THE X-FILES
10:45 – 11:15	почивка	
11:15 – 12:00	проф. д-р Таня Цончева - ИОХЦФ	НОВИ ХОРИЗОНТИ ЗА УСТОЙЧИВО ОПАЗВАНЕ НА ОКОЛНАТА СРЕДА
12:00 – 12:30	гл. ас Катерина Лазарова - ИОМТ	ИНФРАМАТ: МОДЕРНА ИЗСЛЕДО-ВАТЕЛСКА ИНФРАСТРУКТУРА, В ПОДКРЕПА НА НАУКАТА, КУЛТУРАТА И ТЕХНОЛОГИЧНОТО РАЗВИТИЕ
12:30 – 14:00	почивка	
14:00 – 17:00	**Представяния на участниците**	
14:00 – 14:15	Силвия Димова - ИП	ORGANIC-INORGANIC POLYMER HYBRIDS: SYNTHESIS AND APPLICATIONS
14:15 – 14:30	Николай Лумов - ИОХЦФ	ИЗСЛЕДВАНЕ НА ПРЕВРЪЩАНЕТО НА НИТРОБЕНЗИМИДАЗОЛОВИ ПРОИЗ-ВОДНИ В РАДИКАЛ АНИОННИ ПРОДУКТИ: ВЛИЯНИЕ НА ЗАМЕСТИТЕЛИТЕ В БЕНЗИМИДАЗОЛОВИЯ ЦИКЪЛ
14:30 – 14:45	Мария Аргирова - ИОХЦФ	ЕКСПЕРИМЕНТАЛНИ И ТЕОРЕТИЧНИ ИЗСЛЕДВАНИЯ НА РАДИКАЛ-УЛАВЯЩАТА СПОСОБНОСТ НА 2-АМИНО БЕНЗИМИДАЗОЛИЛ ХИДРАЗОНИ
14:45 – 15:00	Пролетина Кардалева - ИОХЦФ	EFFECT OF CONVERSION OF NAPROXEN INTO IONIC LIQUID FORMULATION ON ITS BINDING PROPERTIES TO BOVINE SERUM ALBUMIN
15:00 – 15:15	Силвия Божилова - ИП	ОХАРАКТЕРИЗИРАНЕ НА ЗВЕЗДОВИДНИ ПОЛИ(N-ИЗОПРОПИЛАКРИЛАМИДИ) С ПОТЕНЦИАЛНО БИОМЕДИЦИНСКО ПРИЛОЖЕНИЕ
15:15 – 15:30	Камелия Костова - ХТМУ	ПРОУЧВАНЕ НА ВЛИЯНИЕТО НА МАКРОАКТИВАТОРА ВЪРХУ ФИЗИКОХИМИЧНИТЕ СВОЙСТВА НА БИОРАЗГРАДИМИ СЪПОЛИЕСТЕР-АМИДИ
15:30 – 16:00	почивка	
16:00 – 16:15	Тодор Влахов - ИФТТ	PEO/PVP –БАЗИРАНИ ТВЪРДИ ПОЛИМЕРНИ ЕЛЕКТРОЛИТИ С ГРАФЕНОВ ОКИС
16:15 – 16:30	Катерина Лазарова - ИОМТ	ТЪНКИ ФИЛМИ ОТ СЪПОЛИМЕРИ НА ПВА ДОТИРАНИ СЪС СИЛИКАТНИ НАНОЧАСТИЦИ ЗА ПРИЛОЖЕНИЕ В ОПТИЧНИ СЕНЗОРИ ЗА ВЛАГА

16:30 – 16:45	Анна Атанасова - ИОМТ	СРЕБЪРНИ НАНОЧАСТИЦИ – СИНТЕЗ И ХАРАКТЕРИЗИРАНЕ ЗА ПРИЛОЖЕНИЕ В ПОВЪРХНОСТНО СТИМУЛИРАНА РАМАНОВА СПЕКТРОСКОПИЯ
16:45 – 17:00	Радослав Ангелов - ИОМТ	ВЛИЯНИЕ НА ВИДА НА РАЗТВОРИТЕЛЯ ВЪРХУ ПРОЦЕСА НА ЕЛЕКТРООВЛАКНЯВАНЕ НА ОТПАДЪЧЕН ПОЛИСТИРЕН
23.06.2020		
10:00 – 12:30	**Лекции**	
10:00 – 10:45	проф. д-р Зара Желева – Черкезова - ИК	PREPARATION OF CRITICAL RAW MATERIALS (CRM) - FREE CATALYSTS
10:45 – 11:30	доц. д-р Георги Авдеев - ИФХ	РЕНТГЕНОФАЗОВ АНАЛИЗ – ОСНОВНИ ПОНЯТИЯ
11:30 – 11:45	почивка	
11:45 – 12:30	проф. д-р Даринка Христова - ИП	МАКРОМОЛЕКУЛЕН ДИЗАЙН НА ХИДРОФИЛНИ И АМФИФИЛНИ СЪПОЛИМЕРНИ МРЕЖИ ЗА СПЕЦИФИЧНИ БИОМЕДИЦИНСКИ ПРИЛОЖЕНИЯ
12:30 – 13:30	**почивка**	
13:30 – 16:45	**Представяния на участниците**	
13:30 – 13:45	Катерина Захариева - ИК	PHOTOCATALYTIC MATERIALS FOR DEGRADATION OF DYES UNDER UV-LIGHT
13:45 – 14:00	Радостина Иванова - ИОХЦФ	НАНОСТРУКТУРИРАНИ МЕТАЛООКСИДНИ МАТЕРИАЛИ НА ОСНОВАТА НА ЦЕРИЕВ ОКСИД:ПОЛУЧАВАНЕ, ХАРАКТЕРИЗИРАНЕ И ПРИЛОЖЕНИЕ КАТО КАТАЛИЗАТОРИ ЗА ПЪЛНО ОКИСЛЕНИЕ НА ЕТИЛАЦЕТАТ
14:00 – 14:15	Александра Милева - ИОХЦФ	МЕЗОПОРЕСТИ МЕД-ЦИРКОНИЙ-ТИТАН ОКСИДНИ НАНОКОМПОЗИТИ КАТО КАТАЛИЗАТОРИ ЗА ПОЛУЧАВАНЕ НА ВОДОРОД
14:15 – 14:30	Консолато Росмини (ConsolatoRosmini) - ИОХЦФ	EFFECT OF THE DIFFERENT SYNTHESIS METHODOLOGIES OF FE-CE OXIDE CATALYSTS FORMETHANOL DECOMPOSITION
14:30 – 14:45	Глория Исса - ИОХЦФ	EFFECT OF PREPARATION PROCEDURE ON THE FORMATION OF MESOPOROUS MANGANESIA–CERIA BINARY MATERIALS: PHYSICOCHEMICAL AND CATALYTIC STUDY
14:45 – 15:00	Митко Дойчинов - ИФХ	ПОВЪРХНОСТНИ СВОЙСТВА НА ВОДНИ РАЗТВОРИ НА САПОНИНИ И ТЕХНИ СМЕСИ С ДРУГИ БИОСЪРФАКТАНТИ
15:00 – 15:30	**почивка**	
15:30 – 15:45	Галин Борисов - ИЕЕС	CARBON FREE MEMBRANE ELECTRODE ASSEMBLIES WITH NON – NOBLE CATALYST FOR AEMEC
15:45 – 16:00	Невелин Борисов - ИЕЕС	MULTILAYERED NICKEL BASED ELECTRODES APPLICABLE FOR ADVANCED

		ALKALINE WATER ELECTROLYSER IN A DUAL CELL MODE
16:00 – 16:15	Елица Петкучева - ИЕЕС	INFLUENCE OF THE NICKEL FOAM THICKNESS TO THE ELECTROCHEMICAL PERFORMANCE OF DDM-NF/MxOy ELECTRODES IN ALKALINE MEDIA
16:15 – 16:30	Илиян Попов - ИЕЕС	ВИСОКОЕНЕРГИЙНИ БАТЕРИИ МЕТАЛ – ВЪЗДУХ - ТЕНДЕНЦИИ ЗА РАЗВИТИЕ
16:30 – 16:45	Таня Малакова - ИЕ	НЕУТРОННО И РЕНТГЕНОВИ ДИФРАКЦИОННИ ИЗСЛЕДВАНИЯ НА ИТРИЙ ЗАМЕСТЕН БАРИЕВ ЦЕРАТ
24.06.2020		
10:00 – 12:00	**Лекции**	
10:00 – 10:45	доц. д-р Веселин Тончев – ФзФ, СУ	МОДЕЛИРАНЕ РАЗПРОСТРАНЕНИЕТО НА КОВИД-19: СМЕТАЛОТО НА БОЛЦМАН
10:45 – 11:30	проф. д-р Красимир Темелков - ИФТТ	МОЩНИ АТОМНИ И ЙОННИ ЛАЗЕРИ С ПАРИ НА МЕТАЛИ И МЕТАЛНИ ХАЛОГЕНИДИ, ВЪЗБУЖДАНИ В НАНОСЕКУНДЕН ИМПУЛСЕН НАДЛЪЖЕН РАЗРЯД – РАЗВИТИЕ И ПЕРСПЕКТИВИ
11:30 – 11:40	Г-жа Милена Петкова, фондация „Карол Знание”	Покана за „Предприемачи в науката”
11:40 – 12:00	гл. ас Наталия Берберова – Бухова - ИОМТ	ПРОЕКТ "ОБРАЗОВАНИЕ С НАУКА" - ЕДНА НОВА ВЪЗМОЖНОСТ ЗА ВРЪЗКА МЕЖДУ ОБРАЗОВАНИЕТО И НАУКАТА
12:00 – 13:00	**почивка**	
13:00 – 17:00	**Представяния на участниците**	
13:00 – 13:15	Наталия Берберова – Бухова - ИОМТ	EVALUATION OF OPTICAL RESPONSE OF AZOPOLYMER (PAZO) THIN SOLID FILMS DOPED WITH GOLD NANOPARTICLES
13:15 – 13:30	Радост Иванова - ИМех	РЕОЛОГИЯТА КАТО ИНСТРУМЕНТ ЗА АНАЛИЗ НА СТРУКТУРАТА НА ПОЛИМЕРНИ НАНОКОМПОЗИТИ С ГРАФЕН И ВЪГЛЕРОДНИ НАНОТРЪБИЧКИ
13:30 – 13:45	Вериславъ Ангелов - ИМех	НАНОКОМПОЗИТИ НА БАЗАТА НА ЕПОКСИДНА СМОЛА И ОРГАНОГЛИНА. СТРУКТУРА И НЯКОИ СВОЙСТВА
13:45 – 14:00	Никола Мирчев - ИФХ	СХЕМА НА ХИМИЧНО ПОКРИВАНЕ С МЕТАЛИ НА ЧАСТИЦИ ОТ ЦИРКОНИЕВ ВОЛФРАМАТ
14:00 – 14:15	Илиян Траянов – ХТМУ, ИИХ	NANOMEMBRANE FILTRATION UTILIZATION FOR FERMENTED AND NON-FERMENTED DAIRY PRODUCTS AND BROTHS
14:15 – 14:30	Илиян Траянов – ХТМУ, ИИХ	THERMAL SOLAR DRYERS FOR HOME AND SMALL-PRODUCTION USE WITH PHASE CHANGE MATERIALS AS HEAT STORAGE MEDIA: DESIGN APPROACHES
14:30 – 15:00	**почивка**	

15:00 – 15:15	Роса Гаммелтофт - ИА	ИЗСЛЕДВАНЕ И МОНИТОРИНГ НА ПРОМЕНЛИВОСТТА ПРИ АКТИВНИ ГАЛАКТИЧНИ ЯДРА (ОТ НАО РОЖЕН И АО БЕЛОГРАДЧИК)
15:15 – 15:30	Цветан Цветков - ИА	НАБЛЮДЕНИЕ И ИЗСЛЕДВАНЕ НА СЛЪНЧЕВАТА АКТИВНОСТ
15:30 – 15:45	Галя Петрова - НБУ	ЗНАЧЕНИЕ НА ГЕНЕТИЧНОТО РАЗНООБРАЗИЕ НА РАСТИТЕЛНИ ВИДОВЕ С ПОТЕНЦИАЛНО ПРИЛОЖЕНИЕ ВЪВ ФАРМАЦИЯТА
15:45 – 16:00	Блага Благоева - ИОМТ	АНИЗОТРОПИЯ ИНДУЦИРАНА С УЛТРАВИОЛЕТОВА СВЕТЛИНА ВЪВ ФТАЛИМИДНИ 2-ХИДРОКСИ ШИФОВИ БАЗИ
16:00 – 16:15	Ирник Дионисиев - ИОМТ	2D ПЛАТИНОВ ДИСЕЛЕНИД: СИНТЕЗ И ПРИЛОЖЕНИЯ
16:15 – 16:30	Джихан Менсеидов - ИМех	ПРИЛОЖЕНИЕТО НА 3Д ПЕЧАТА В СУПЕРКОНДЕНЗАТОРИТЕ
16:30 – 17:00	доц. д-р Даниела Карашанова - ИОМТ	Закриване на 13 Пролетен семинар

EFFECT OF CONVERSION OF NAPROXEN INTO IONIC LIQUID FORMULATION ON ITS BINDING PROPERTIES TO BOVINE SERUM ALBUMIN

Proletina Kardaleva, Maya Guncheva

Institute of Organic Chemistry with Centre of Phytochemistry, BAS ,
Acad. G. Bonchev № 9 Str., Sofia-1113, Bulgaria
e-mail: pkardaleva@orgchm.bas.bg

Conversion of the hydrophobic solid drugs into ionic liquid (IL) formulation may offer some advantages such as enhanced water solubility, a new route of application, enhanced cell or receptor selectivity, etc. It can help to overcome the problem with polymorphism of the crystal compounds and therefore to ensure higher therapeutic safety and effectiveness of the drug.

In the focus of this study is the interaction of bovine serum albumin (BSA) with a series of ILs containing an anion naproxenate (NPX) and cations, short-chain alcohol amino acid esters, namely L-valine ethyl ester [ValOEt] (1), L-valine propyl ester [L-ValOPr] (2), L-isopropyl ester [L-ValOiPr] (3), L-valine butyl ester [L-ValOBut] (4) and L-leucine ethyl ester [L-LeuOEt] (5). It is noteworthy to be mentioned that the interactions with the drugs with serum albumins influence their pharmacokinetics and pharmacodynamics as well as their bioavailability, toxicity, and therapeutic effect.

The thermodynamic parameters for the interactions of NPX and NPX-based ILs with BSA are determined by isothermal titration calorimetry (ITC) at 25ºC. The determined dissociation constants (Kd) are between 64 and 281 nM. The negative values of free energy (ΔG_0) and enthalpy (ΔH_0) is indicative that the binding of all tested compounds to BSA is spontaneous and exothermic. Except for [ValOiPr][NPX], NPX-BSA and IL-BSA characterize with $\Delta H_0 < 0$ and entropy (ΔS_0) < 0, which is an indication that the van der Waals interactions and H-bonding are predominant for these compounds. Interestingly, the binding of [ValOiPr][NXP] is mainly driven by electrostatic interactions. For the latter, we found that the stoichiometric binding number (n) is 2, while n is 1 for the NPX, 1 and 5, and 0.8 for the compounds 2 and 4.

Using FTIR spectroscopy we monitored the induced conformation changes in BSA due to the binding of NXP and the series of ILs. Rearrangements in BSA are observed in the presence of the compounds, but as a whole, the structure of BSA is preserved. In the presence of ValOPr-NPX and LeuOEt-NPX the structure of BSA seems more open and the side chains are exposed to the surface. In the presence of the ValOiPr-NPX, we observed an increase in α-helical content, probably the structure of BSA becomes more compact.

Acknowledgements: This work was supported by the Bulgarian Ministry of Education and Science under the National Research Programme "Young scientists and postdoctoral students" approved by DCM # 577 / 17.08.2018.

Keywords: naproxen-based ionic liquids; bovine serum albumin; ligand-protein interactions; ITC; FTIR

RESEARCH INFRASTRUCTURE IN SUPPORT OF SCIENCE, TECHNOLOGY AND CULTURE

Scientific conference

Sofia, September, 29-30, 2020

On-line meeting

Study of the Conformation and Thermal Stability of Bovine Serum Albumin in Complexes with Ionic Liquids Containing Naproxen Anion

P. Kardaleva[1], S. Todinova[2], D. Yancheva[1], M. Guncheva[1]

[1]*Institute of Organic Chemistry with Centre of Phytochemistry, BAS, Acad. G. Bonchev Str. Bl. 9, 1113 Sofia, Bulgaria,*
[2]*Institute of Biophysics and Biomedical Engineering, BAS, Acad. G. Bonchev Str. Bl. 21, 1113 Sofia, Bulgaria*
e-mail: pkardaleva@orgchm.bas.bg

Ionic liquids (ILs) are salts containing asymmetric organic cations and organic or nonorganic anion. ILs based on active pharmaceutical ingredients are interesting for the pharmaceutical industry because based on their specific structure they have the potential to overcome some problems of solid-state drugs. Naproxen (NPX) is a non-steroidal drug with anti-inflammatory, antipyretic, and analgesic activities with low solubility and bioavailability. Conversion of the drug in ionic liquid formulation improves its physicochemical characteristics and possibly bioavailability. Serum albumin is the main transport protein of the drug in mammals. The focus of this study is a series of ILs containing cations esters of amino acids and NPX anion and their complex with bovine serum albumin (BSA).

We applied attenuated total reflectance Fourier deconvoluted infrared spectroscopy (ATR-FTIR) to observe the effect of the NPX-ILs on the BSA secondary structure. For all tested compounds, in the Amide I region (1600-1700 cm -1) we observed the typical bands for α-helices, β-sheets, unordered structures and in some cases aggregates. In the presence of NPX the secondary structure of BSA is slightly unfolded, but as a whole, the structure is similar to that of the native protein in solution. In the BSA-ILs complexes we observed decreasing of α-helical structures and increasing of β-structures and in some cases, side chains of BSA backbone are exposed to the surface and i.e. the BSA molecule becomes more open. The observed conformational changes are in agreement with the changes in the thermal stability of BSA-IL complexes monitored by differential scanning calorimetry (DSC). Three transitions slightly shifted (by 2-3ºC) toward the higher temperatures were observed in the DSC curves of the BSA-IL complexes. Annealing of the DSC curves shows that for each complex the three transitions are characterized by different enthalpy, which suggests that depending on their structures, probably ILs are bound in a different pocket in BSA.

Acknowledgments: This work was partially supported by the Bulgarian Ministry of Education and Science under the National Research Program “Young scientist and postdoctoral Students” approved by DSM # 577/ 17.08.2018.
Research equipment of distributed research infrastructure INFRAMAT (part of Bulgarian National roadmap for research infrastructures) supported by Bulgarian Ministry of Education and Science under contract D01-284/17.12.2019 was used in this investigation.

Декларация

Във връзка избягване на двойно финансиране по Национална програма „Млади учени и постдокторанти“, приета с РМС 577/17.08.2018 г.

Аз, долуподписаният[i] (акад. длъжност, научна степен, име, презиме, фамилия),

Биолог, Пролетина Красимирова Кардалева

в качеството си на участник в Национална програма „Млади учени и постдокторанти“ в периода 01.04.2021-31.12.2021, декларирам, че :

не получавам ***възнаграждение от други източници*** за изпълняваните от мен дейности по програмата и не се предвижда да получавам, включително и по процедури: „Изграждане и развитие на центрове по компетентност“, „Изграждане и развитие на центрове за върхови постижения“, Национални научни програми, както и други национални източници или източници от чужбина.

Известно ми е, че за деклариране на неверни данни нося наказателна отговорност по Наказателния кодекс.

Декларатор: 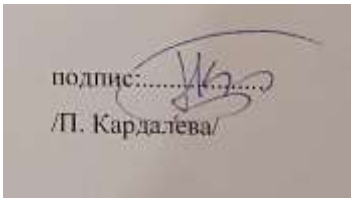

(Име, фамилия, подпис)

Дата04.02.2021

[i]